

The Different Physical Mechanisms that Drive the Star-Formation Histories of Giant and Dwarf Galaxies

C. P. Haines,¹ A. Gargiulo,^{1,2} F. La Barbera,¹ A. Mercurio,¹ P. Merluzzi,¹ and G. Busarello¹

¹*INAF - Osservatorio Astronomico di Capodimonte, via Moiariello 16, I-80131 Napoli, Italy; chris@na.astro.it*

²*Department of Physics, Università Federico II, Napoli, Italy*

1 February 2008

ABSTRACT

We present an analysis of star-formation and nuclear activity in galaxies as a function of both luminosity and environment in the fourth data release of the Sloan Digital Sky Survey (SDSS DR4). Using a sample of 27 753 galaxies in the redshift range $0.005 < z < 0.037$ that is $\gtrsim 90\%$ complete to $M_r = -18.0$ we find that the $\text{EW}(\text{H}\alpha)$ distribution is strongly bimodal, allowing galaxies to be robustly separated into passively-evolving and star-forming populations about a value $\text{EW}(\text{H}\alpha) = 2\text{\AA}$. In high-density regions $\sim 70\%$ of galaxies are passively-evolving independent of luminosity. In the rarefied field however, the fraction of passively-evolving galaxies is a strong function of luminosity, dropping from 50% for $M_r \lesssim -21$ to zero by $M_r \sim -18$. Indeed for the lowest luminosity range covered ($-18 < M_r < -16$) none of the ~ 600 galaxies in the lowest density quartile are passively-evolving. The few passively-evolving dwarf galaxies in field regions appear as satellites to bright ($\gtrsim L^*$) galaxies. We find a systematic reduction of $\sim 30\%$ in the $\text{H}\alpha$ emission from dwarf ($-19 < M_r < -18$) star-forming galaxies in high-density regions with respect to field values, implying that the bulk of star-forming dwarf galaxies in groups and clusters are currently in the process of being slowly transformed into passive galaxies. The fraction of galaxies with optical AGN signatures decreases steadily from $\sim 50\%$ at $M_r \sim -21$ to $\sim 0\%$ by $M_r \sim -18$ closely mirroring the luminosity-dependence of the passive galaxy fraction in low-density environments. This result reflects the increasing importance of AGN feedback with galaxy mass for their evolution, such that the star-formation histories of massive galaxies are primarily determined by their past merger history. In contrast, the complete absence of passively-evolving dwarf galaxies more than ~ 2 virial radii from the nearest massive halo (i.e. cluster, group or massive galaxy) indicates that internal processes, such as merging, AGN feedback or gas consumption through star-formation, are not responsible for terminating star-formation in dwarf galaxies. Instead the evolution of dwarf galaxies is primarily driven by the mass of their host halo, probably through the combined effects of tidal forces and ram-pressure stripping.

Key words: galaxies: active — galaxies: clusters: general — galaxies: dwarf — galaxies: evolution — galaxies: stellar content

1 INTRODUCTION

It has been known for decades that local galaxies can be broadly divided into two distinct populations (e.g. Hubble 1926, 1936; Morgan 1958; de Vaucouleurs 1961). The first are red, passively-evolving, bulge-dominated galaxies dominated by old stellar populations that make up the red sequence; and the second make up the “blue cloud” of young, star-forming, disk-dominated galaxies (e.g. Strateva et al. 2001; Kauffmann et al. 2003a,b;

Blanton et al. 2003b; Baldry et al. 2004; Driver et al. 2006; Mateus et al. 2006).

It has also long been known that the environment in which a galaxy inhabits has a profound impact on its evolution in terms of defining both its structural properties and star-formation histories (e.g. Hubble & Humason 1931). In particular, passively-evolving spheroids dominate cluster cores, whereas in field regions galaxies are typically both star-forming and disk-dominated (Blanton et al. 2005a). These differences have

been quantified through the classic morphology–density (Dressler 1980) and star-formation (SF)–density relations (Lewis et al. 2002; Gómez et al. 2003). However, despite much effort (e.g. Treu et al. 2003; Balogh et al. 2004a,b; Gray et al. 2004; Kauffmann et al. 2004; Tanaka et al. 2004; Christlein & Zabludoff 2005; Rines et al. 2005; Baldry et al. 2006; Blanton, Berlind & Hogg 2006; Boselli & Gavazzi 2006; Haines et al. 2006a,b; Mercurio et al. 2006; Sorrentino, Antonuccio-Delogo & Rifatto 2006; Weinmann et al. 2006a,b; Mateus et al. 2007), it still remains unclear whether these environmental trends are: (i) the direct result of the initial conditions in which the galaxy forms, whereby massive galaxies are formed earlier preferentially in the highest overdensities in the primordial density field, and have a more active merger history, than galaxies that form in the smoother low-density regions; or (ii) produced later by the direct interaction of the galaxy with one or more aspects of its environment, whether that be other galaxies, the intracluster medium (ICM), or the underlying dark-matter distribution (e.g. tidal stripping). Several physical mechanisms have been proposed that could cause the transformation of galaxies through interactions with their environment such as ram-pressure stripping (Gunn & Gott 1972), galaxy harassment (Moore et al. 1996), and suffocation (also known as starvation or strangulation) in which the diffuse gas in the outer galaxy halo is stripped preventing further accretion onto the galaxy before the remaining cold gas in the disk is slowly consumed through star-formation (Larson, Tinsley & Caldwell 1980).

The morphologies and star-formation histories of galaxies are also strongly dependent on their masses, with high-mass galaxies predominately passively-evolving spheroids, and low-mass galaxies generally star-forming disks. A sharp transition between these two populations is found about a characteristic stellar mass of $\sim 3 \times 10^{10} M_{\odot}$, corresponding to $\sim M^* + 1$ (Kauffmann et al. 2003a,b). This bimodality implies fundamental differences in the formation and evolution of high- and low-mass galaxies. The primary mechanism behind this transition appears to be the increasing efficiency and rapidity with which gas is converted into stars for more massive galaxies according to the Kennicutt-Schmidt law (Kennicutt 1998; Schmidt 1959). This results in massive galaxies with their deep potential wells consuming their gas in a short burst ($\lesssim 2$ Gyr) of star-formation at $z > 2$ (Chiosi & Cararro 2002), while dwarf galaxies have much more extended star-formation histories and gas consumption time-scales longer than the Hubble time (van Zee 2001).

In the monolithic collapse model for the formation of elliptical galaxies this naturally produces the effect known as “cosmic downsizing” whereby the major epoch of star-formation occurs earlier and over a shorter period in the most massive galaxies and progressively later and over more extended time-scales towards lower mass galaxies. This has been confirmed observationally both in terms of the global decline of star-formation rates in galaxies since $z \sim 1$ (Noeske et al. 2007a,b) and the fossil records of low-redshift galaxy spectra (Heavens et al. 2004; Panter et al. 2007). Finally in analyses of the absorption lines of local quiescent galaxies, the most massive galaxies are found to have higher mean stellar ages and abundance ratios than their lower mass counterparts, indicating that they formed stars earlier and over shorter time-scales (Thomas et al. 2005;

Nelan et al. 2005). In this scenario, the mass-scale at which a galaxy becomes quiescent should decrease with time, with the most massive galaxies becoming quiescent earliest, resulting in the red sequence of passively-evolving galaxies being built up earliest at the bright end (Tanaka et al. 2005), and the evolving mass-scale of E+A (post-starburst) galaxies (Poggianti et al. 2004).

However the standard paradigm for the growth of structure and the evolution of massive galaxies within a CDM universe is the hierarchical merging scenario (e.g. White & Rees 1978; Kauffmann, White & Guideroni 1993; Lacey & Cole 1993) in which massive elliptical galaxies are assembled through the merging of disk galaxies as first proposed by Toomre (1977) (for a full historical review of this subject see Struck 2006). Although downsizing appears at first sight to be at odds with the standard hierarchical model for the formation and evolution of galaxies, Merlin & Chiosi (2006) are able to reproduce the same downsizing as seen in the earlier “monolithic” models in a hierarchical cosmological context, resulting in what they describe as a revised monolithic scheme whereby the merging of substructures occurs early in the galaxy life ($z > 2$). Further contributions to cosmic downsizing and the observed bimodality in galaxy properties could come from the way gas from the halo cools and flows onto the galaxy (Dekel & Birnboim 2006; Kereš et al. 2005) and which affects its ability to maintain star-formation over many Gyr, in conjunction with feedback effects from supernovae and AGN (e.g. Springel et al. 2005a; Croton et al. 2006). These mechanisms which can shut down star-formation in massive galaxies allow the hierarchical CDM model to reproduce very well the rapid early formation and quenching of stars in massive galaxies (e.g. Bower et al. 2006; Hopkins et al. 2006b, 2007b; Birnboim, Dekel & Neistein 2007). In particular, the transition from cold to hot accretion modes of gas when galaxy halos reach a mass $\sim 10^{12} M_{\odot}$ (Dekel & Birnboim 2006) could be responsible for the observed sharp transition in galaxy properties with mass.

If the evolution of galaxies due to internal processes is effectuated earlier and more rapidly with increasing mass, then this would give less opportunity for external environmental processes to act on massive galaxies. Moreover, low-mass galaxies having shallower potential wells are more susceptible to disruption and the loss of gas due to external processes such as ram-pressure stripping and tidal interactions. This suggests that the relative importance of internal and external factors on galaxy evolution and on the formation of the SF-, age- and morphology-density relations could be mass-dependent, in particular the relations should be stronger for lower mass galaxies. Such a trend has been observed by Smith et al. (2006) who find that radial age gradients (out to $1 R_{\text{vir}}$) are more pronounced for lower mass ($\sigma < 175 \text{ km s}^{-1}$) cluster red sequence galaxies than their higher mass subsample.

The environmental trends of fainter galaxies ($M_r \gtrsim M^* + 1$) have generally been examined using galaxy colours as a measure of their star formation history. Whereas the colour of massive galaxies becomes steadily redder with increasing density, a sharp break in the mean colour of faint galaxies is observed at a critical density corresponding to $\sim R_{\text{vir}}$ (Gray et al. 2004; Tanaka et al. 2004). In a photometric study of galaxies in the environment

of the Shapley supercluster core, we found that the fraction of faint ($M^* + 2 < M_r < M^* + 6$) red galaxies dropped from $\sim 90\%$ in the cluster cores to $\sim 20\%$ by the virial radius (Haines et al. 2006a), while the shape of the faint end of the red galaxy luminosity function changes dramatically with density inside the virial radius (Mercurio et al. 2006).

In Haines et al. (2006b, hereafter Paper I) we investigated the possible mass-dependency of the age-density and SF-density relations by comparing the global trends with environment for giant ($M_r < -20$) and dwarf ($-19 < M_r < -17.8$) galaxies in the vicinity of the $z = 0.03$ supercluster centred on the rich cluster A2199, the richest low-redshift ($z < 0.05$) structure covered by the Sloan Digital Sky Survey (SDSS) DR4 spectroscopic dataset.

A strong bimodality was seen in the mean stellar age- M_r distribution about a mean stellar age of 7 Gyr, with a population of bright (L^*) galaxies ~ 10 Gyr old, and a second population of fainter galaxies dominated by young ($\lesssim 3$ Gyr) stars, while a clear age-density distribution was identified for both giant and dwarf subsamples. We confirmed the findings of Smith et al. (2006) that the age-density relation is stronger for dwarf galaxies, while the critical density at which the ages increase markedly is higher for dwarf galaxies, occurring at values typical of the cluster virial radius. In the highest-density regions we found that $\gtrsim 80\%$ of both giant and dwarf subsamples were old (> 7 Gyr). However, whereas the fraction of old giant galaxies declines gradually with decreasing density to the global field value of $\sim 50\%$, that of dwarf galaxies drops rapidly, tending to *zero* for the lowest density bins. Identical trends with density were independently observed when passive galaxies were identified from their lack of H α emission.

Looking directly at the spatial distribution of galaxies in the vicinity of the supercluster, in field regions the giant population shows a completely interspersed mixture of both young and old populations, indicating that their evolution is driven primarily by their merger history rather than direct interactions with their environment. In contrast, the mean stellar ages of dwarf galaxies were strongly correlated with their immediate environment: those passively-evolving or old dwarf galaxies found outside of the rich clusters were always found within poor groups or as a satellite to an old, giant ($\gtrsim L^*$) galaxy. No isolated old or passively-evolving dwarf galaxies were found.

In this article we extend the study to cover the entire SDSS DR4 footprint, creating a volume-limited sample of $\sim 28\,000$ galaxies with $0.005 < z < 0.037$ that is $\gtrsim 90\%$ complete to $M_r = -18$ ($M^* + 3.2$). We reexamine the arguments of Paper I taking advantage of this much larger dataset to provide quantitative measures of the environmental dependencies on star-formation in galaxies and in particular how these vary with the galaxy mass/luminosity. We attempt to disentangle the different contributions to the SF-density relation caused by physical mechanisms internal to the galaxy (e.g. AGN feedback) and those caused by the direct interaction of the galaxy with its surroundings (for a review of how the diverse mechanisms leave different imprints on the environmental trends see e.g. Treu et al. 2003).

In § 2 we describe the dataset used, the classification of galaxies, and the measures used to remove any biases due to aperture effects and the complex survey geometry, while in § 3 we describe the adaptive kernel method used

to define the local galaxy density. In § 4 we quantify how the fraction of passively-evolving galaxies depends on both environment and mass/luminosity, while in § 5 we examine the ongoing effects of environment on galaxies that are still forming stars. In § 6 we examine which aspects of environment are most important for defining the star-formation history of galaxies in field regions, in particular whether the presence of a nearby galaxy of a particular mass has any role in star-formation being truncated in a galaxy. In § 7 we quantify the fraction of galaxies having AGN signatures as a function of both luminosity and environment, and examine the possible connection between AGN feedback and the shut-down of star-formation in galaxies. In § 8 we compare our results with predictions from the semi-analytic models of Croton et al. (2006). In § 9 we discuss the possible physical mechanisms that can affect star-formation in galaxies and produce the observed environmental trends, and finally in § 10 we present a summary of our results and conclusions. Throughout we assume a concordance Λ CDM cosmology with $\Omega_M = 0.3$, $\Omega_\Lambda = 0.7$ and $H_0 = 70 \text{ km s}^{-1} \text{ Mpc}^{-1}$.

2 THE DATA

The sample of galaxies used in this work is taken from the fourth release of Sloan Digital Sky Survey (SDSS DR4; Adelman-McCarthy et al. 2006) an imaging and spectroscopic survey covering an area of π sr principally located in the North Galactic Cap (York et al. 2000). The area covered by the imaging survey has a total extension of 6670 square degrees, from which *ugriz* broad band imaging data have been acquired for 180 million objects.

Instead of the spectroscopic catalogue obtained with the SDSS reduction and calibration procedures, we refer to the low redshift catalogue (LRC) taken from the New York University Value Added Galaxy Catalogue (NYU-VAGC) of Blanton et al. (2005c). The LRC is a catalogue of SDSS galaxies with $0.0033 < z < 0.05$, $r_{\text{Petro}} < 18$ and with $\mu_{50} < 24.5 \text{ mag arcsec}^{-2}$ in the *r*-band (where μ_{50} is the surface brightness within a circular aperture containing half of Petrosian flux). Blanton et al. (2005c) also perform some further quality control checks on the catalogues, including: a procedure for dealing with large, complex galaxies that were incorrectly deblended by the SDSS pipeline, and correctly associating spectra from fibres that were offset from the actual centres of the objects; bringing into the LRC a number of galaxies with redshifts but morphologically classified as stars; and finally performing a number of visual checks on objects in the catalogue. In addition, Blanton et al. (2005c) computed the *K*-correction for each object of the NYU-VAGC using the version 3.2 of the software K-CORRECT (Blanton et al. 2003c) providing in this way, the absolute magnitudes of the objects.

The region covered by the SDSS survey in this release includes two wide contiguous regions in the North Galactic Cap, one centred roughly on the Celestial Equator and the other around $\delta = +40^\circ$, both with $120^\circ < \alpha < 240^\circ$, and three narrower stripes, one centred on the Celestial Equator again, and two at $\delta = +15^\circ$ and $\delta = -10^\circ$ with $-60^\circ < \alpha < 60^\circ$. We have excluded the LRC galaxies belonging to the three stripes as the computation of local galaxy density could be

biased due to the narrow dimension of these regions (no point is more than 3.4 Mpc from the boundary).

In this paper we focus our attention particularly on the environmental impact on the dwarf galaxy population. Hence we have only selected from the LRC the galaxies with $0.005 < z < 0.037$ in order to obtain a catalogue which is $\gtrsim 90\%$ complete to $M_r < -18$ ($M_r \lesssim M^* + 3$) yielding a final catalogue of 27 753 objects. The lower limit in redshift at $z = 0.005$ is due both to the peculiar velocities which can seriously influence the distance estimates and to the great problems arising from the deblending of the large and re-solved objects.

As dwarf galaxies tend to have low surface brightnesses, it is important to consider whether significant numbers of dwarf galaxies are missing from the SDSS spectroscopic catalogue (and hence ours) due to surface brightness selection effects, which are three-fold: (i) photometric incompleteness; (ii) galaxies not being targetted due to being shredded by the deblending algorithm; (iii) targetted galaxies which did not yield reliable redshifts. Blanton et al. (2005b) analysed the surface brightness completeness of the LRC up to $\mu_{50} < 24.5$ and found that for $M_r < -18.0$ the LRC does not suffer from significant ($\gtrsim 10\%$) incompleteness due to surface brightness effects. At fainter magnitudes they find that although low-surface brightness dwarf galaxies are clearly detectable in the SDSS images, the photometric pipeline tended to mistakenly deblend them or overestimate the background sky levels.

2.1 Spectral indices of the galaxies

The stellar indices used are taken from MPA/JHU SDSS DR4 catalogues (Kauffmann et al. 2003a, hereafter K03), in which a continuum fitting code was adopted that was optimized to work with SDSS data in order to recover also the weak features of the spectra and to account for the Balmer absorption (Tremonti et al. 2004). The library of spectra templates are composed of single stellar population models following the assumption that the star-formation history of a galaxy is made up of a set of discrete bursts. The models are based on new population synthesis code of Bruzual & Charlot (2003) which incorporates a spectral library covering the 3200–9300 Å range and with high resolution (3 Å) matching the SDSS data. The templates span a wide set of ages and metallicities. After a Gaussian convolution of the templates in order to match the stellar velocity dispersion of each galaxy, the best fitting model is constructed by performing a non-negative least-squares fit with the dust extinction values A_z of K03 and the $\lambda^{-0.7}$ attenuation law of Charlot & Fall (2000). K03 use the amplitude of the 4000 Å break (as defined in Balogh et al. 1999) and the strength of the H δ_A absorption line as diagnostics of the stellar populations of the galaxies, from which maximum-likelihood estimates of the z -band mass-to-light ratios are made. These in conjunction with the z -band absolute magnitude and the dust attenuation A_z yield the stellar mass \mathcal{M} of each galaxy.

The stellar mass estimates of K03 are only available for galaxies in the range $14.5 < r < 17.77$. For the remainder of the galaxies we use the same technique as Baldry et al. (2006) who estimate the stellar mass-to-light ratio of each galaxy from its $u - r$ colour, using the analysis

of Bell & de Jong (2001) who show that for models of star-forming disk galaxies with reasonable metallicities and star-formation histories, the stellar mass-to-light ratios correlate strongly with the colours of the integrated stellar populations. Briefly, for each 0.05 mag bin in $u - r$ we determine the median value of (\mathcal{M}/L_r) for those galaxies with stellar mass estimates by K03, and linearly interpolating between bins, create a relation between the $u - r$ colour and its stellar mass-to-light ratio. This relation is then used to estimate stellar masses for the remaining galaxies from their r -band luminosity and $u - r$ colour.

2.2 Aperture biases

Throughout this article we quantify the current star-formation and nuclear activity in our sample of galaxies from their spectral indices, in particular their H α emission. One possible cause of bias in estimating the star-formation rate of galaxies in our sample is due to the galaxy spectrum being obtained through a 3 arcsec diameter aperture rather than over the full extent of the galaxy. Significant radial star-formation gradients are possible within galaxies, particularly those undergoing nuclear star-bursts or spiral galaxies with a prominent passively-evolving bulge, that can result in the “global” star-formation rate being significantly over or underestimated based upon spectra containing flux dominated by the galaxy nucleus. Kewley, Jansen & Geller (2005) indicate that star-formation rates based on spectra obtained through apertures covering less than $\sim 20\%$ of the integrated galaxy flux can be over or underestimated by a factor ~ 2 , and to ensure the SDSS fibres sample more than this 20% require galaxies to be at $z > 0.04$. Clearly in order to use the SDSS dataset to study star-formation in $M_r \sim -18$ galaxies this is not possible, as at $z = 0.04$ they are already too faint to be included in the SDSS spectroscopic sample. Brinchmann et al. (2004) quantify the effects of aperture bias on their estimates of star-formation rates in SDSS galaxies, and find that indeed in the case of galaxies with $\mathcal{M} \gtrsim 10^{10.5} M_\odot$ strong trends are apparent when plotting SFR/\mathcal{M} as a function of redshift (their Fig. 13), the star-formation rate being systematically underestimated for galaxies at the lowest redshifts by as much as a factor three. However they also find that for lower-mass galaxies, which cover the same redshift range as our dataset, the aperture biases are considerably smaller ($\lesssim 20\%$) and a simple scaling of the fiber SFR by the r -band flux, as done by Hopkins et al. (2003), is perfectly acceptable.

In a subsequent paper (Haines et al. 2007, Paper III) we perform a complementary analysis of the same volume-limited sample combining the SDSS r -band photometry with *GALEX* NUV imaging to obtain *integrated* measures of recent star-formation in ~ 15 per cent of our galaxies. A comparison of the integrated NUV $- r$ colours with the SDSS fiber spectral indices allows us to quantify the effects of aperture bias within our sample. We find that for $M_r < -20$ galaxies aperture biases are significant with ~ 7 per cent of galaxies classified as passive ($\text{EW}[\text{H}\alpha] < 2 \text{ \AA}$) from their spectra yet also having blue colours ($\text{NUV} - r \lesssim 4$) indicative of recent star-formation. As expected, many of these galaxies appear as face-on spiral galaxies with prominent bulges. This fraction drops to zero at fainter magnitudes ($M_r \gtrsim -19.5$) as the SDSS fibres cover a greater fraction

of the galaxies, while lower luminosity galaxies tend to be either late-type spirals or dwarf ellipticals. The luminosity function of early-type spirals (Sa+b) for which aperture biases are by far the most important has a Gaussian distribution centred at $M_r \sim -21.7$ and width $\sigma \sim 0.9$ mag (de Lapparent 2003), and hence are rare at $M_r \gtrsim -20$.

We thus indicate that star-formation rate estimates for $M_r > -20$ galaxies in our sample based on H α fluxes obtained through the SDSS fibres should be reasonably robust against aperture biases. In the case of $M_r < -20$ galaxies where aperture biases are important, we limit our analysis to that based on the simple separation of passive and star-forming galaxies, and where possible refer to comparable studies performed using samples limited to redshifts where aperture effects are much reduced (e.g. Gómez et al. 2003; Balogh et al. 2004a; Tanaka et al. 2004). Throughout this article we indicate the possible effects of aperture biases on our results.

2.3 The completeness of the catalogue

The completeness (i.e. the fraction of galaxies brighter than the SDSS spectroscopic magnitude limit of $r = 17.77$ that have been spectroscopically observed resulting in good redshifts) of our catalogue is strictly influenced by three factors: i) The dimension of the fibres which prevents two objects closer than $55''$ from being observed. Roughly 6% of the objects are not spectroscopically observed for this reason (Blanton et al. 2003a).

ii) The blending of bright galaxies with saturated stars. Bright galaxies which overlap saturated stars are flagged themselves as SATURATED and hence will not be targeted spectroscopically. As one goes to fainter magnitudes the blending goes down as the area covered by the galaxy decreases. The fraction of galaxies not targeted for spectroscopy for this reason rises from 1% overall to 5% at the bright end of galaxy sample ($r < 15$) (Strauss et al. 2002).

iii) The selection criteria set by LRC are broader than those of the selection algorithm used to target galaxies for the spectroscopic SDSS survey (Strauss et al. 2002).

The pronounced incompleteness of the spectroscopic catalogue at the bright end may bias the detection and characterization of low- z groups of galaxies, since the most luminous objects of these structures are not included. To cope with this deficiency, we have matched the photometric catalogue of SDSS with the NASA/IPAC Extragalactic Database (NED). For all the objects with a positive match we have associated the SDSS *ugriz* photometry with the corresponding redshift from NED and calculated the absolute magnitudes. There are a total of 803 galaxies added this way to our catalogue with $0.005 < z < 0.037$ and $r < 17.77$. Their contribution is largest at bright magnitudes where the 202 $r < 14.5$ galaxies from NED make up $\sim 8\%$ of the catalogue. We do not have the spectral indices for the galaxies taken from NED, and so they are only used here in defining the local environment of the LRC galaxies.

Despite the contribution from NED, our improved spectroscopic catalogue is still incomplete. To compute the completeness, assuming that in the catalogue all the objects with spectra are correctly classified, it is firstly necessary to check the classification of the objects without spectra. From a first visual check on the limited sample of bright

galaxies ($r < 14.5$) with no spectra we found many objects such as saturated stars and satellite tracks classified as galaxies. To remove these objects from our photometric catalogue in the most automatic way, we have compared their flags with those of known galaxies (i.e. with redshifts) looking for some peculiar differences. From this comparison we have noticed that, differently from galaxies, all the saturated stars have the flags SATURATED, SATUR_CENTER and the great part of those due to satellite tracks have the flag EDGE (Stoughton et al. 2002). After removing the objects with these flags, we have performed a visual inspection of a subsample of galaxies in the range $14.5 < r < 17.7$ which were not targetted for spectroscopy. In this subsample we found that the photometric pipeline sometimes fails the detection, recognizing non-existent objects. Real $r < 17.7$ galaxies should be clearly detected also in at least the g , i and z images, whereas this should not be the case for non-existent objects, and hence to exclude these objects we have only selected galaxies as having $g, i, z < 21$ and $r < 17.77$ the last limit due to the selection criteria of the SDSS spectroscopic survey. Finally, in the photometric catalogue we also found a small percentage ($\sim 1\%$) of stars classified as galaxies and of badly deblended objects. Since no particular flag characterizes them and it being impossible to reject these by hand we have left these objects in the catalogue their influence on determining the completeness being negligible.

To compute the completeness of this *cleaned* catalogue we have followed the prescription of Blanton et al. (2003a) based on the algorithm used by SDSS to locate the plates and to assign the fibres. This procedure places on the area covered by the survey a set of $1^\circ 49'$ radius circles (defined tiles) such to maximize the number of available fibres. The intersection between the tiles and the survey region defines a set of spherical polygons. The union of all the polygons that could have been observed by a unique set of tiles is called “sector”. These sectors are the regions over which we have computed the completeness, \mathcal{C} , as the fraction of galaxies in the cleaned photometric catalogue that have good redshifts.

3 DEFINITION OF ENVIRONMENT

To study how the evolution of galaxies is related to their local environment, we firstly need to define the environment by means of the local number density of $M_r < -18$ galaxies.

To compute the local number density $\rho(\mathbf{x}, z)$ we use a variant of the adaptive kernel estimator (Silverman 1986; Pisani 1993, 1996) where each galaxy i with $M_r < -18$ is represented with an adaptive Gaussian kernel $\kappa_i(\mathbf{x}, z)$ in redshift space. Differently from Silverman (1986) and its previous applications to astronomical data (e.g. Haines et al. 2004a,b, 2006a) in which the kernel width σ_i is iteratively set to be proportional to $\rho_i^{-1/2}$, we fix the radial width to 500 km s^{-1} and the transverse width σ_i to $(8/3)^{1/2} D_3$, where D_3 is the distance of the third nearest neighbour within 500 km s^{-1} , a limit which includes $\sim 99\%$ of physical neighbours (as determined from the Millenium simulation considering the three nearest galaxies in real-space) and minimizes the contamination of background galaxies. The choice of D_3 was made to maximize the sensitivity of the density estimator to poor groups containing as few as four galaxies, while the $(8/3)^{1/2}$ smoothing factor was added to

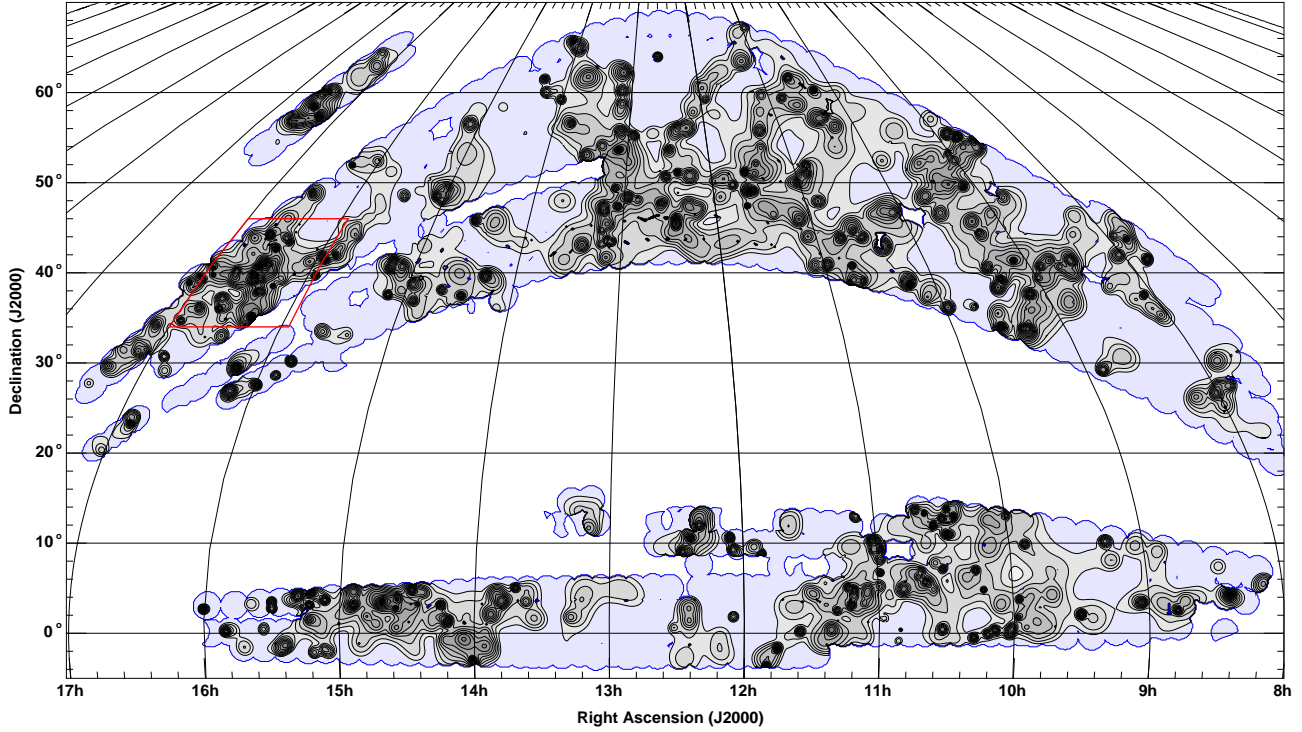


Figure 1. Luminosity-weighted density map of $M_r < -18$ galaxies over the redshift range $0.023 < z < 0.037$ over the entire SDSS DR4 North Galactic Cap region. The isodensity contours are logarithmically spaced, the spacing between each contours indicating a factor $\sqrt{2}$ increase in the r -band luminosity-weighted local density. The red box indicates the $12^\circ \times 12^\circ$ region containing the $z = 0.03$ A2199 supercluster analysed in Paper I.

reduce the noise of the estimator, so that in “field” regions $\sigma_i \approx D_8$ which, as shown in Appendix A and Table A1, appears the optimal value for the smoothing length-scale.

The choice both of the method and of the kernel dimensions is designed to resolve the galaxy’s environment on the scale of its host dark matter halo, as it is the mass of its host halo and whether the galaxy is the central or a satellite galaxy, that is believed to be the dominant factor in defining its global properties such as star-formation history or morphology (e.g. Lemson & Kauffmann 1999; Kauffmann et al. 2004; Yang et al. 2005; Blanton et al. 2006). In the case of galaxies within groups or clusters, the local environment is measured on the scale of their host halo (0.1–1 Mpc), while for galaxies in field regions the local density is estimated by smoothing over its 5–10 nearest neighbours or scales of 1–5 Mpc.

For each galaxy i the local galaxy density is defined as:

$$\rho_i(\mathbf{x}, z) \propto \sum_j \eta_j \exp \left[-\frac{1}{2} \left\{ \left(\frac{D_{ij}}{\sigma_j} \right)^2 + \left(\frac{\nu_i - \nu_j}{500 \text{ km s}^{-1}} \right)^2 \right\} \right] \quad (1)$$

where $\eta_j = C_j^{-1} (2\pi)^{-3/2} \sigma_j^{-2}$ is the normalization factor, D_{ij} is the projected distance between the galaxies i and j , ν_i is the recession velocity of galaxy i , and the sum is over all galaxies with $M_r < -18$. Note that we also calculate the local galaxy density for galaxies fainter than $M_r = -18$.

We have performed a number of tests of the efficiency of this density estimator, in particular with regard to identifying group and isolated field galaxies, by applying the estimator to the public galaxy catalogues from the Millennium simulation (Springel et al. 2005c), and comparing it

to other estimators based on the nearest-neighbour algorithm as applied by Balogh et al. (2004b, hereafter BB04) and Baldry et al. (2006, hereafter BB06). These tests are described in detail in the Appendix, and confirm that the estimator is at least as efficient as any variant of the nearest-neighbour algorithm for the same dataset. In particular the estimator is very sensitive to the presence of even poor groups containing as few as four galaxies, the result being that selecting galaxies with $\rho < 0.5 \text{ Mpc}^{-2} (500 \text{ km s}^{-1})^{-1}$ a pure field sample is produced, with *no* contamination from group members. In contrast 90% of $\rho > 4$ galaxies lie within the virial radius of a galaxy group or cluster, while those galaxies in the transition regions between groups and field environments ($r \sim R_{\text{vir}}$) have densities in the range $1 \lesssim \rho \lesssim 4$.

Figure 1 shows the resultant r -band luminosity-weighted density map for galaxies with $M_r < -18$ over the redshift range $0.023 < z < 0.037$ for the whole SDSS DR4 North Galactic Cap region. For comparison, the red box indicates the $12^\circ \times 12^\circ$ region containing the A2199 supercluster that was analysed in Paper I. The adaptive kernel estimator used has the advantage of being able to be used as a group-finder (e.g. Bardelli et al. 1998; Haines et al. 2004a), by identifying groups and clusters as local maxima in the galaxy density function $\rho(\mathbf{x}, z)$, and as demonstrated in the Appendix all groups and clusters having four or more $M_r < -18$ galaxies in the SDSS DR4 catalogue will be marked by local maxima in the density map of Figure 1. To put this in perspective, we are sensitive to environments comparable to the Local Group (which contains four $M_r < -18$ galaxies: Milky Way, LMC, M31 and M33) and the other nearby groups (the M81, Cen A/M83 and Maf-

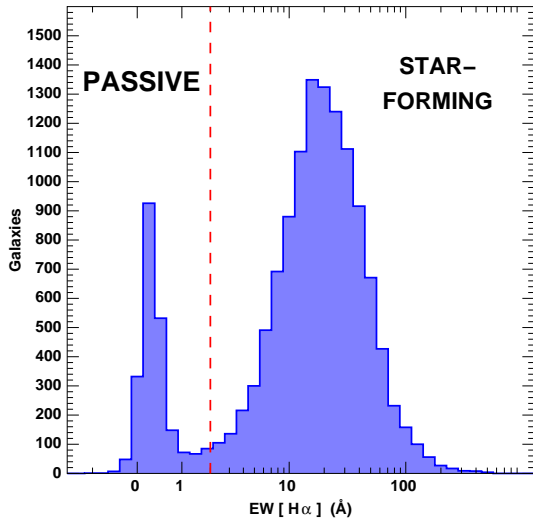


Figure 2. The $\text{EW}(\text{H}\alpha)$ distribution of $M_r < -18.0$ galaxies (AGN excluded) in the redshift range $0.005 < z < 0.037$.

fei groups; Karachentsev 2005). Such poor groups represent the preferential major-merger mass scale ($M_{\text{halo}} \sim 10^{12} M_{\odot}$ for galaxies of stellar mass $\sim 10^{10} - 10^{11} M_{\odot}$ (Hopkins et al. 2007a).

4 THE BIMODALITY IN $\text{EW}(\text{H}\alpha)$ AND ITS DEPENDENCE ON LUMINOSITY AND ENVIRONMENT

One of the best understood and calibrated indicators of the star-formation rate (SFR) in galaxies is the $\text{H}\alpha$ nebular emission-line, whose luminosity is directly proportional to the ionizing radiation from massive ($> 10 M_{\odot}$) short-lived (< 20 Myr) stars, and hence the $\text{H}\alpha$ emission provides a near-instantaneous measure of the current star-formation rate (Kennicutt 1998). Figure 2 shows the $\text{EW}(\text{H}\alpha)$ distribution of $M_r < -18.0$ galaxies in the redshift range $0.005 < z < 0.037$ from the SDSS DR4 spectroscopic dataset. The x-axis is scaled as $\sinh^{-1} \text{EW}(\text{H}\alpha)$: this results in the scale being linear at $\text{EW}(\text{H}\alpha) \approx 0 \text{ \AA}$ where measurement errors dominate, and logarithmic for $\text{EW}(\text{H}\alpha) \gtrsim 10 \text{ \AA}$ allowing the lognormal distribution of equivalent widths for star-forming galaxies to be conveniently displayed.

We exclude galaxies showing an AGN signature, as their $\text{H}\alpha$ emission may be dominated by emission from the AGN rather than star-formation. AGN are defined using the $[\text{N II}]\lambda 6584 / \text{H}\alpha$ versus $[\text{O III}]\lambda 5007 / \text{H}\beta$ diagnostics of Baldwin, Phillips, & Terlevich (1981) as lying above the 1σ lower limit of the models defined by Kewley et al. (2001). When either the $[\text{O III}]\lambda 5007$ or $\text{H}\beta$ lines are unavailable ($\text{S/N} < 3$), the two-line method of Miller et al. (2003) is used, with AGN identified as having $\log([\text{N II}]\lambda 6584 / \text{H}\beta) > -0.2$. We also exclude those galaxies without an $\text{H}\alpha$ measurement.

The distribution is clearly bimodal, with two approximately Gaussian distributions: one that is narrow and centred at $\text{EW}(\text{H}\alpha) \sim 0.2 \text{ \AA}$, corresponding to passively-evolving galaxies with little or no ongoing star-formation; and another that is wider and centred at $\text{EW}(\text{H}\alpha) \sim 20 \text{ \AA}$, corre-

sponding to galaxies currently actively star-forming. Mid-way between these two distributions there are relatively-speaking very few galaxies, and we identify the dividing line between passive and star-forming galaxies as being $\text{EW}(\text{H}\alpha) = 2 \text{ \AA}$, that corresponds approximately to the minimum in the distribution between the two peaks. Note that this value is different to that used in the studies of Balogh et al. (2004a, hereafter B04) and Tanaka et al. (2004, hereafter T04) who use $\text{EW}(\text{H}\alpha) = 4 \text{ \AA}$ to separate passive and star-forming galaxies, but is the same as used by Rines et al. (2005, hereafter R05). The lower value however appears justified empirically from Fig. 2, and is sufficiently large that even for the faintest galaxies ($r \sim 17.77$) the limit still represents a 4σ detection in $\text{H}\alpha$, the median uncertainty in $\text{EW}(\text{H}\alpha)$ only reaching 0.5 \AA by $r = 17.77$. The inclusion of galaxies with optical AGN signatures would tend to fill in the gap in the bimodal distribution, their $\text{H}\alpha$ equivalent widths typically in the range $0.5 - 10 \text{ \AA}$ (median = 1.56 \AA).

The left panel of Fig. 3 shows how the bimodality in $\text{EW}(\text{H}\alpha)$, and hence the ongoing star-formation rate of galaxies, depends on both luminosity and environment. Each coloured curve shows the fraction of passively-evolving galaxies ($\text{EW}(\text{H}\alpha) < 2 \text{ \AA}$) as a function of local density for a particular luminosity range as indicated. The lowest luminosity bin ($-18 < M_r < -16$) is far from complete, and is biased heavily towards galaxies close to the bright magnitude limit, but the environmental trends should be representative of those galaxies slightly fainter than $M_r = -18$. Galaxies that lie very close to the edge of the SDSS DR4 footprint are likely to have biased density estimates, and so galaxies that are within 2 Mpc or σ_i Mpc, whichever is smaller, of the survey boundary are excluded from all further analyses. This results in a final sample of 22 113 galaxies.

At the highest densities ($\rho \gtrsim 5$), corresponding to the centres of galaxy clusters or groups, passive galaxies dominate for the entire luminosity range studied, with $\sim 70\%$ of galaxies being passive independent of luminosity. At lower densities in contrast the fraction of passive galaxies depends strongly on luminosity. Even at densities comparable to those seen at the virial radius of groups/clusters, the fraction of $M_r \gtrsim -20$ galaxies that are passive has dropped to $\sim 20\%$ or lower, while that of brighter galaxies has dropped only slightly. The luminosity dependence is greatest for the lowest density regions corresponding to field environments well beyond the environmental influence of galaxy clusters or groups. Here the fraction of passive galaxies drops from $\sim 50\%$ for $M_r \lesssim -21$ galaxies to $\sim 0\%$ for $M_r \gtrsim -19$. In the lowest luminosity bin ($-18 < M_r < -16$) the passive galaxy fraction has dropped to precisely zero in the lowest density regions. In fact, there are no passive galaxies in the lowest density quartile, corresponding to $\simeq 600$ galaxies in total.

These results can be compared with the analysis of BB04 who show in their Fig. 2 the fraction of red sequence galaxies as a function of both environment and r -band luminosity using data from SDSS DR1. As here, BB04 find that $\sim 70\%$ of galaxies in their highest density bin belong to the red sequence. However, in their lowest density bin, the luminosity dependence is somewhat less than presented here, dropping from $\sim 35\%$ for $-22 < M_r < -21$ to $\sim 8\%$ for $-19 < M_r < -18$.

The right panel of Fig. 3 repeats the analysis using stellar mass (\mathcal{M}) instead of r -band luminosity. Essen-

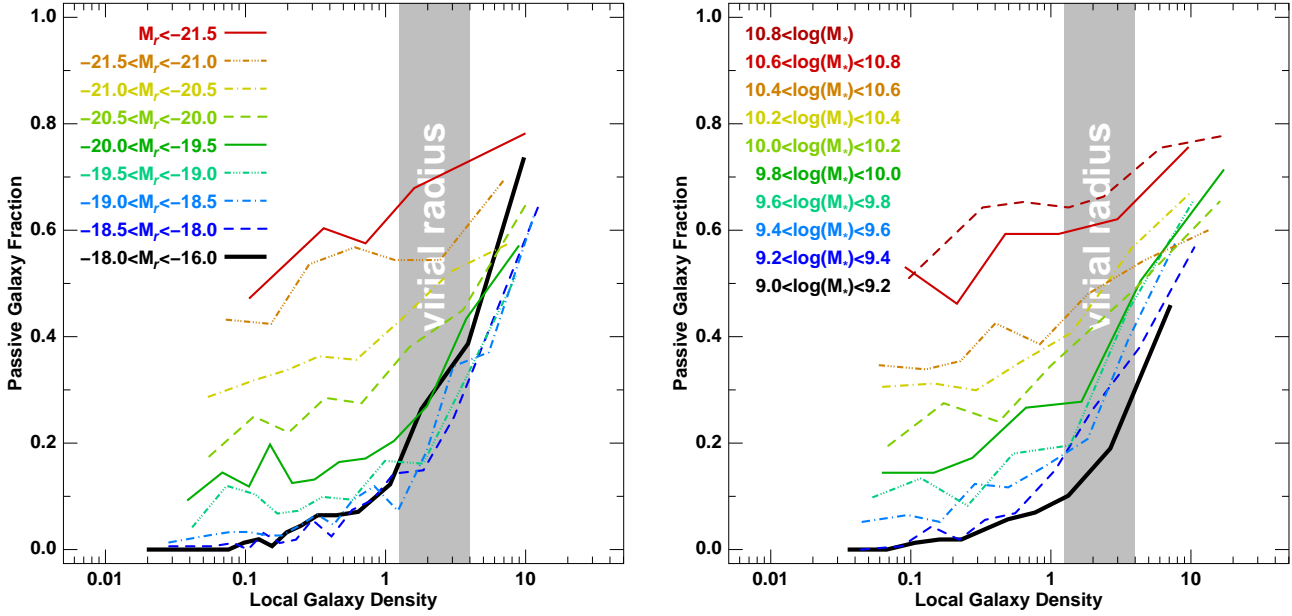


Figure 3. The fraction of passively-evolving galaxies ($\text{EW}[\text{H}\alpha] < 2 \text{ \AA}$) as a function of both local density and luminosity (left panel) or stellar mass (right panel). Each coloured curve corresponds to a different luminosity / stellar mass bin as indicated. Each density bin contains 150 galaxies. The grey shaded region indicates the typical densities found for galaxies near the virial radius ($0.8 < (r/R_{\text{vir}}) < 1.2$) of groups or clusters in the Millennium simulation (see Fig. A1).

tially the same results are obtained, with passive galaxies dominating in high-density regions independent of stellar mass, while in low-density regions the fraction of passively-evolving galaxies depends strongly on stellar mass, dropping from $\sim 50\%$ at $\mathcal{M} \sim 10^{10.8} M_\odot$ to zero by $\mathcal{M} \sim 10^{9.2} M_\odot$. We note that for stellar masses below $10^{9.2} M_\odot$ we are no longer volume-limited introducing a selection bias, whereby passively-evolving galaxies are more likely to be missed by the $r = 17.77$ magnitude limit than star-forming galaxies of the same mass and at the same distance.

BB06 have performed a very similar analysis of the same SDSS DR4 dataset, examining how the fraction of *red sequence* galaxies varies as a function of both environment and stellar mass (their Fig. 11a). They consider a much larger volume than our analysis, resulting in a significantly larger sample, particularly at the high-mass end, allowing them to follow the environmental trends for stellar mass bins to $\log \mathcal{M} = 11.6$. BB06 use a different approach to K03 to calculate the mass-to-light ratios of the galaxies based on the $u - r$ colour only, but they use the same IMF, and as shown in Fig. 5 of BB06 obtain stellar masses that on average are within 0.1 dex of one another. The global trends are qualitatively the same, with red sequence galaxies dominating in high-density environments independently of stellar mass, while in the lowest density environments the fraction of red sequence galaxies is a strong function of stellar mass. This latter trend extends to the higher stellar masses studied by BB06, falling from $\sim 100\%$ at $\log \mathcal{M} \sim 11.6$ to 5% by $\log \mathcal{M} \sim 9.0$. However for the same stellar mass bin, the red sequence fractions of BB06 in low-density regions are systematically $\sim 10\%$ higher than the passive galaxy fraction from our analysis.

Although the trends shown here in Fig. 3 are similar to those of BB04 and BB06, as discussed above there are some important differences. In particular, we find that for

$M_r \gtrsim -18.0$ or $\mathcal{M} \lesssim 10^{9.2} M_\odot$ there are no passively-evolving galaxies in the lowest-density bins, whereas for the same stellar mass / luminosity ranges both BB04 and BB06 find that 5–10% of the galaxies belong to the red sequence in their lowest density bin. This difference has important consequences for the conclusions that can be drawn from the data (see § 9). What is the cause of this remnant population of faint red galaxies in low-density environments, that disappears in our analysis? Firstly, as discussed previously, the local density estimator used in BB04 and BB06 is not completely able to separate group and field galaxies, so that even for the lowest density bin considered $\sim 5\%$ of the galaxies are group members, the majority of which lie on the red sequence at all luminosities. Secondly, not all red sequence galaxies are passively-evolving: a significant fraction are known to be star-forming, and appear red due to high levels of dust extinction. In an analysis of the SDSS main sample galaxies covered by infrared imaging from the SWIRE survey, Davoodi et al. (2006) find that 17% of red sequence galaxies are dusty star-forming galaxies (identified by their high $24\mu\text{m}$ to $3.6\mu\text{m}$ flux ratios and $\text{H}\alpha$ emission), while Wolf et al. (2005) find that dusty star-forming galaxies constitute more than one-third of the red sequence population in the A901/2 supercluster region.

Conversely, due to the SDSS spectra being obtained through $3''$ diameter fibres, the region covered may only cover the central bulge region of nearby large galaxies, resulting in galaxies appearing passive despite having normal star-forming disks. As discussed earlier (§ 2.2) based on a comparison of the SDSS and *GALEX* NUV photometry of $\sim 15\%$ (4065 galaxies) of our low-redshift sample we find that $\sim 8\%$ (20 out of 246) of bright ($M_r < -21$) galaxies are classified as passive yet have blue UV-optical colours ($\text{NUV} - r < 4$) indicative of normal star-forming galaxies (Paper III). This fraction drops steadily with magnitude

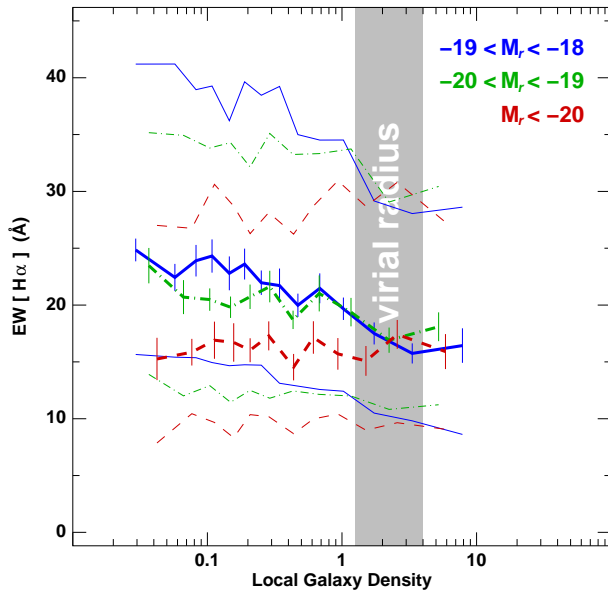


Figure 4. The dependence of $\text{EW}(\text{H}\alpha)$ on local density for star-forming galaxies with $\text{EW}(\text{H}\alpha) > 2\text{\AA}$. The red dashed lines represent giant galaxies ($M_r < -20$), the green dot-dashed lines represent galaxies with $-20 < M_r < -19$, while the blue solid lines represent dwarf galaxies ($M_r > -19$). The thick and thin lines show respectively the median and interquartile values of the distribution. The median lines are accompanied by 1σ error limits estimated by bootstrap resampling including the measured error in $\text{EW}(\text{H}\alpha)$. Each bin contains 300 galaxies.

(being 2.5% for $-21 < M_r < -20$ galaxies), falling to zero (0 out of 1375) for galaxies at $M_r \gtrsim -19.5$. We find no significant variation of these fractions with environment. We thus indicate that the passive galaxy fractions obtained for the higher luminosity/mass bins are overestimated due to aperture effects, but that those for the lower luminosity galaxies ($M_r \gtrsim -20$) are robust against aperture biases.

5 STAR-FORMING GALAXIES

If star-forming galaxies at the present day are affected by environmental mechanisms when they move from low- to high-density regions, we should see a signature of this transformation which depends on the relevant time-scale. In particular, if the dominant environmental mechanism produces a gradual ($\gtrsim 1$ Gyr) decline in star-formation when galaxies become bound to groups or clusters (e.g. suffocation), then star-forming galaxies in dense regions should show systematically lower star-formation rates or $\text{EW}(\text{H}\alpha)$. On the other hand, if the dominant environmental mechanism suppresses star-formation in galaxies on a very short timescale, then we should not expect any significant changes in the $\text{EW}(\text{H}\alpha)$ distribution of star-forming galaxies, since the galaxies will quickly become classed as passive and hence not contribute to the $\text{EW}(\text{H}\alpha)$ distribution. In the previous studies of B04 and T04 the distributions of $\text{EW}(\text{H}\alpha)$ of giant ($M_r < M^* + 1$) star-forming ($\text{EW}(\text{H}\alpha) > 4\text{\AA}$) galaxies show no dependence on local density, while R05 found no difference in the $\text{EW}(\text{H}\alpha)$ distributions of star-forming galaxies inside the virial radius, in infall regions ($1 < (r/R_{200}) < 5$) or in field

regions. From these results they imply that few giant galaxies can be currently undergoing a gradual decline in star-formation due to environmental processes. However, when considering fainter galaxies with $M^* + 1 < M < M^* + 2$ T04 found the $\text{EW}(\text{H}\alpha)$ of star-forming galaxies to be slightly smaller in dense regions, a result taken to be a signature of the slow truncation of star-formation in faint galaxies.

5.1 $\text{H}\alpha$ -density relation for star-forming galaxies

Following B04 and T04 we show in Fig. 4 the $\text{EW}(\text{H}\alpha)$ distribution of star-forming galaxies as a function of local density for three luminosity ranges: $M_r < -20$ (red dashed lines) which can be compared with the results of B04 ($M_B < -20.2$; $M_r < -21.3$) or the bright sample of T04 ($M_r < -20.3$); $-19 < M_r < -20$ (green dot-dashed lines) which is comparable to the faint sample of T04; and $-18 < M_r < -19$ (blue solid lines). In each case, star-forming galaxies are defined as having $\text{EW}(\text{H}\alpha) > 2\text{\AA}$ as throughout this article. Note that both B04 and T04 use $\text{EW}(\text{H}\alpha) > 4\text{\AA}$, but using this value instead makes no noticeable difference to the results. We also exclude here those galaxies classified as AGN. As observed in previous studies, there is no apparent dependence on density for the $\text{EW}(\text{H}\alpha)$ distribution for galaxies with $M_r < -20$. In contrast, the trends for lower luminosity galaxies show a significant drop in $\text{EW}(\text{H}\alpha)$ with increasing density, most of the drop occurring within the range $0.5 \lesssim \rho \lesssim 2$ which represents the transition between galaxies inside and outside bound structures. The significance of the trends are measured using the Spearman rank correlation test and reported in Table 5.1. Whereas the $\text{EW}(\text{H}\alpha)$ distribution of $M_r < -20$ star-forming galaxies shows no correlation with local density ρ , significant anti-correlations are found for the $-20 < M_r < -19$ and $-19 < M_r < -18$ star-forming galaxy populations at the 5σ and 10σ level respectively.

We do not expect aperture biases to have any significant effects on the environmental trends presented here, as we observe no dependencies on local galaxy density for the distribution of SDSS fiber aperture covering fractions in any of the luminosity ranges. Similarly we find no environmental trends for the fraction of the early-type spiral galaxies classified as passive from their SDSS spectra yet having blue $\text{NUV}-r$ colours. The only possible effect could be a systematic underestimation of the $\text{H}\alpha$ emission in the $M_r < -20$ luminosity bin, but our results for this bin are fully consistent with the comparable trends obtained by T04 and B04 based upon galaxy samples at $0.03 < z < 0.065$ and $0.05 < z < 0.095$ respectively, where aperture effects should not be important (Kewley et al. 2005).

To see exactly how the distribution of $\text{EW}(\text{H}\alpha)$ changes with environment, Fig. 5 shows the $\text{EW}(\text{H}\alpha)$ distribution of galaxies in high ($\rho > 1.0$; red histogram) and low ($\rho < 0.5$; blue dashed histogram) density environments for three luminosity ranges, corresponding to $M_r < -20$ (left panel), $-20 < M_r < -19$ (middle) and $-19 < M_r < -18$ (right). The vertical red and blue dotted lines indicate the median values of star-forming galaxies ($\text{EW}(\text{H}\alpha) > 2\text{\AA}$).

The bimodal character of the $\text{EW}(\text{H}\alpha)$ distribution is apparent in both the high- and low-density environments for each of the luminosity ranges studied. The two environmental dependencies described in Figs. 3 and 4 can both

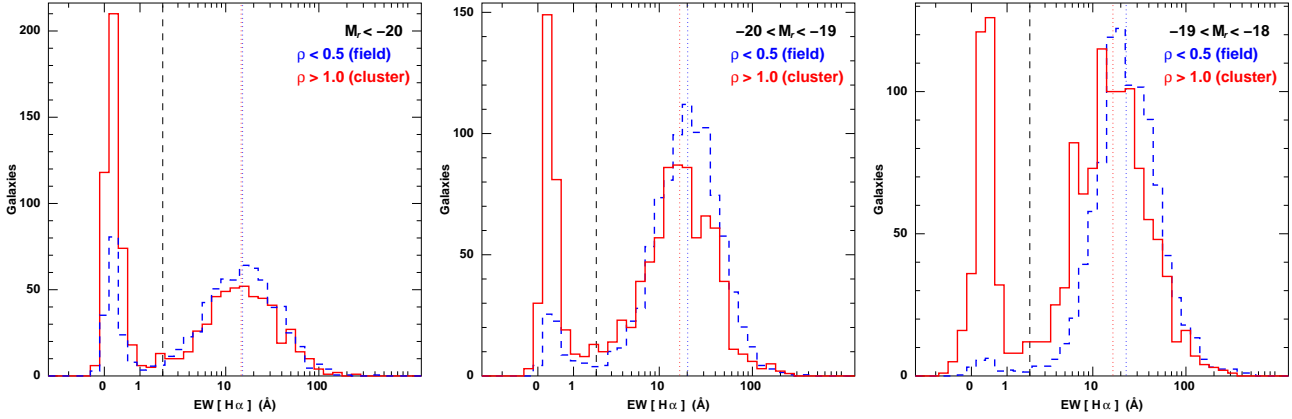


Figure 5. A comparison of the $\text{EW}(\text{H}\alpha)$ distributions for galaxies in high- ($\rho > 1.0$; red histogram) and low-density ($\rho < 0.5$; blue dashed histogram) regions for three luminosity ranges, corresponding to $M_r < -20$ (left panel), $-20 < M_r < -19$ (middle) and $-19 < M_r < -18$ (right). The vertical scale corresponds to the number of galaxies per bin in the high-density histogram, while the low-density histogram has been scaled to allow comparison of the distribution of star-forming galaxies. The red and blue dotted lines indicate the median values of star-forming galaxies ($\text{EW}[\text{H}\alpha] > 2 \text{ \AA}$) in the high- (red) and low-density (blue) regions.

Magnitude range	Median $\text{EW}[\text{H}\alpha](\text{\AA})$		Probability (Kolmogorov-Smirnov)	U test (σ)	Spearman rank correlation ρ
	$\rho < 0.5$	$\rho > 1.0$			
$M_r < -20$	15.19	14.66	0.464	0.07	0.0102 ± 0.0242
$-20 < M_r < -19$	20.23	16.58	2×10^{-6}	5.26	-0.0753 ± 0.0179
$-19 < M_r < -18$	22.85	16.48	6×10^{-25}	11.27	-0.1580 ± 0.0156

Table 1. Comparison of the $\text{EW}(\text{H}\alpha)$ distributions in high ($\rho > 1.0$) and low ($\rho < 0.5$) density environments.

be seen when comparing the $\text{EW}(\text{H}\alpha)$ distributions for the high- and low-density environments.

Firstly, a global shift in the relative fractions of star-forming and passively-evolving galaxies is apparent. The two histograms have been normalized so that distributions of the star-forming galaxies appear to have approximately the same height. As a result, the relative increase in the fraction of passively-evolving galaxies from low- to high-density environments is clear. This relative increase is strongly dependent on luminosity, rising from about a factor 2.5–3 for luminous ($M_r < -20$) galaxies to a factor ~ 20 for the dwarf ($-19 < M_r < -18$) galaxy population.

The second effect can be seen as a global shift in the $\text{EW}(\text{H}\alpha)$ distribution of the star-forming galaxies from high- to low-density environments. In each environment and luminosity range, the $\text{EW}(\text{H}\alpha)$ distribution of the star-forming galaxies can be well described as being log-normal (and hence appearing as a Gaussian distribution in the figure). However, whereas there is no apparent difference in the high- and low-density distributions for luminous ($M_r < -20$) star-forming galaxies, at lower luminosities, the high-density $\text{EW}(\text{H}\alpha)$ distributions are *systematically* shifted to lower values than their low-density counterparts. The level of this shift is quantified by comparison of the median values of the distribution, while the significance of the differences between the two distributions are estimated through application of the non-parametric Kolmogorov-Smirnov and Wilcoxon-Mann-Whitney U tests, the results of which are shown in Table 1. These results confirm that while the $\text{EW}(\text{H}\alpha)$ distribution of the high- and low-density $M_r < -20$ galaxy populations are fully consistent with one another,

for the lower luminosity samples the null hypothesis that the high- and low-density star-forming populations have the same $\text{EW}(\text{H}\alpha)$ distribution is rejected at very high significance levels. For the $-19 < M_r < -18$ sample, the $\text{H}\alpha$ emission from star-forming galaxies in high-density environments is systematically lower by $\sim 30\%$ with respect to their low-density counterparts.

The $\text{H}\alpha$ emission (and hence star-formation) must be suppressed in a significant fraction of galaxies when they fall into a cluster or group for the first time. However, for these galaxies to remain classed as star-forming, this suppression must act over a long period of time, to allow a significant fraction of galaxies to be seen in the process of transformation into passively-evolving galaxies. If we assume that the $\text{H}\alpha$ emission of galaxies declines exponentially with time as they are being transformed, and that the rate at which galaxies are transformed remains constant, the $\text{EW}(\text{H}\alpha)$ of galaxies which are *currently* in the process of being transformed but are still classed as star-forming, will drop from $\sim 20 \text{ \AA}$ to 2 \AA , with an average of $\sim 8 \text{ \AA}$. Hence star-forming galaxies in the process of transformation will have *on average* $\sim 40\%$ of their emission prior to their being transformed. To produce a global systematic reduction of $\sim 30\%$ in the $\text{H}\alpha$ emission would then require $\sim 50\%$ of the dwarf star-forming galaxies in high-density regions to be in the process of being transformed into passive galaxies. Given that, as discussed previously, as many as 30–40% of galaxies in the high-density do not lie within the virialized regions of a cluster or group, this suggests that the vast majority of dwarf star-forming galaxies in groups or clusters are *currently* in the process of being transformed into passive galaxies.

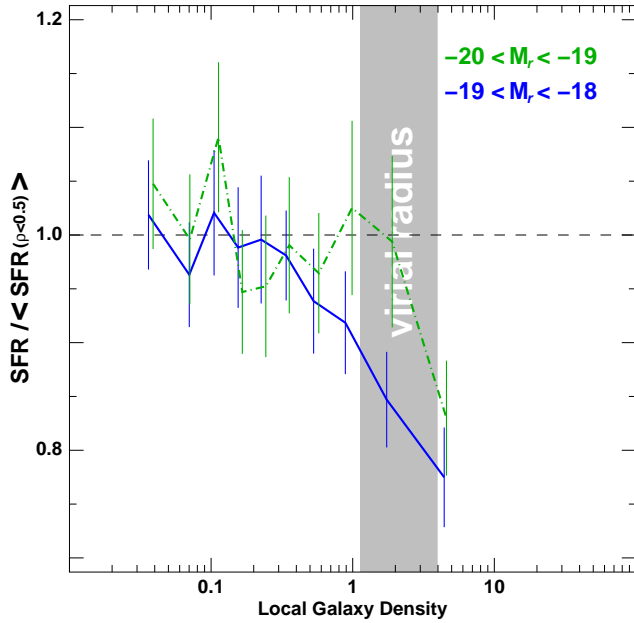


Figure 6. The dependence of the median star-formation rate on local density for star-forming galaxies with $\text{EW}(\text{H}\alpha) > 2\text{\AA}$. The green dot-dashed lines represent galaxies with $-20 < M_r < -19$, while the blue solid lines represent dwarf galaxies ($M_r > -19$). The lines are accompanied by 1σ error limits estimated by bootstrap resampling and include the measured error in $\text{EW}(\text{H}\alpha)$ and uncertainties in the level of dust obscuration. Each bin contains 300 galaxies.

Magnitude range of galaxies	Median SFR ($\text{M}_{\odot}\text{yr}^{-1}$)		P(K-S)	U test (σ)
	$\rho < 0.5$	$\rho > 1.0$		
$-20 < M_r < -19$	0.496	0.443	0.0079	2.30
$-19 < M_r < -18$	0.191	0.157	7×10^{-9}	6.52

Table 2. Comparison of the SFRs of star-forming galaxies in high ($\rho > 1.0$) and low ($\rho < 0.5$) density environments.

5.2 SFR-density relation for star-forming galaxies

The current star-formation rate of a galaxy can be estimated from its $\text{H}\alpha$ flux through the calibration given by Kennicutt (1998):

$$\text{SFR} (\text{M}_{\odot}\text{yr}^{-1}) = \frac{L(\text{H}\alpha)}{1.27 \times 10^{34} \text{W}} \quad (2)$$

Before applying this calibration, it is necessary to correct for the effects of dust obscuration and account for the effects of emission lost by virtue of the spectra being obtained through a fibre whose aperture may be significantly smaller than the galaxy. The obscuration correction is measured by the Balmer decrement, estimated by measuring the ratio of the stellar absorption-corrected $\text{H}\alpha$ and $\text{H}\beta$ line fluxes, and assuming case B recombination and the obscuration curve of Cardelli, Clayton & Mathis (1989). The aperture correction is quantified as the ratio of the observed r -band Petrosian flux and the continuum flux at the wavelength of $\text{H}\alpha$ within the fibre aperture. A full discussion of these corrections and the use of $\text{H}\alpha$ line emission as

a SFR indicator in SDSS data is given in Hopkins et al. (2003) where the explicit calculation used is given as equation B2. Moustakas, Kennicutt & Tremonti (2006) compare the integrated SFRs estimated from the $\text{H}\alpha$ flux using the above procedure with those estimated from IRAS infra-red data and find the two estimates consistent with a precision of $\pm 70\%$ and no systematic offset, confirming that the extinction-corrected $\text{H}\alpha$ luminosity can be used as a reliable SFR tracer, even for the most dust-obscured systems. Using the above calibration and corrections, we plot in Fig. 6 the median SFR of star-forming galaxies as a function of local density for galaxies in the luminosity range $-20 < M_r < -19$ (green dot-dashed line) and $-19 < M_r < -18$ (blue solid line). As discussed in §2.2 aperture effects will strongly bias the estimates of star-formation rates made using the method of Hopkins et al. (2003) for the most massive galaxies in our sample and so we do not plot the results for $M_r < -20$ galaxies. To allow the effect of high-density environments on star-formation to be measured, each curve is normalized to the median SFR of “field” ($\rho < 0.5$) star-forming galaxies in the same luminosity range.

The environmental trends in SFR broadly match those shown earlier in Fig. 4 for the $\text{EW}(\text{H}\alpha)$ distribution of star-forming galaxies, confirming that those trends do indeed reflect changes in the global SFR with environment, and are not due to variations in dust obscuration or aperture biases. These trends are quantified in Table 2 which compares the median SFRs of star-forming galaxies in high- and low-density environments for both luminosity ranges, as well as estimates the significance of any differences. The most significant result ($\sim 6\sigma$) is the observed systematic drop of $\sim 20\%$ in the median SFR of dwarf ($-19 < M_r < -18$) star-forming galaxies in high-density regions with respect to field galaxies. In both luminosity bins there appears a systematic drop in SFR for densities greater than 1Mpc^{-2} , which suggests that star-formation is suppressed in a significant fraction of galaxies when they infall for the first time into a cluster or group.

As discussed earlier we do not expect aperture biases to be important for galaxies in these luminosity bins. Moreover we find no dependencies on local galaxy density for the fraction of galaxy flux covered by the SDSS fiber apertures in either luminosity bin.

As a final check to confirm that aperture effects are not behind the observed environmental trends in $\text{EW}(\text{H}\alpha)$ and star-formation rates, we repeat the analyses using galaxy $u-r$ colours as a measure of their current/recent star-formation. The $u-r$ colours are determined over apertures defined by the Petrosian radius, and hence represent an integrated measure of a galaxy’s star-formation history. The resultant trends in the median $u-r$ colour with local density for each of the luminosity ranges are presented in Fig. 7.

For each of the three luminosity ranges star-forming galaxies become increasingly redder with density. The strength of the trend increases with decreasing luminosity from 0.07 mag for $-21 < M_r < -20$ galaxies to $\sim 0.2 \text{mag}$ for $M_r > -20$ galaxies. Almost identical trends were observed by Balogh et al. (2004b) for galaxies selected as star-forming by their $u-r$ colour. In the case of the two lower luminosity ranges ($M_r > -20$) the bulk of the change in $u-r$ colour with density occurs at $\rho > 1$, as seen for the trend in SFR of Fig. 6. These trends are fully consistent with those

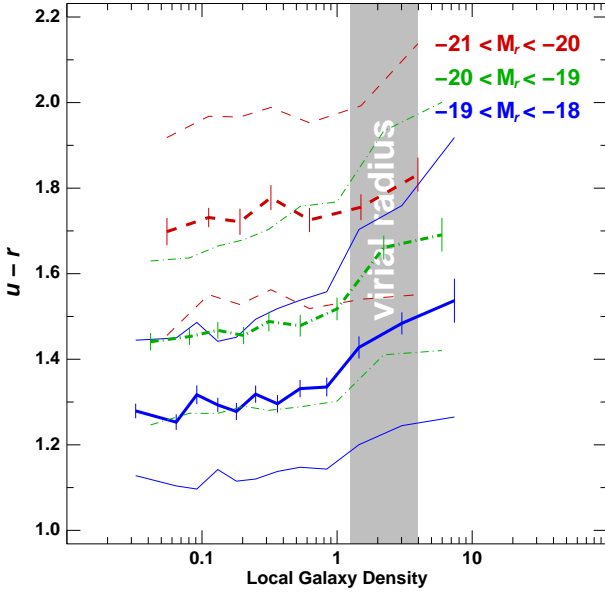


Figure 7. The dependence of the $u - r$ galaxy colour on local density for star-forming galaxies with $\text{EW}(\text{H}\alpha) > 2\text{\AA}$. The red dashed lines represent giant galaxies ($M_r < -20$), the green dot-dashed lines represent galaxies with $-20 < M_r < -19$, while the blue solid lines represent dwarf galaxies ($M_r > -19$). The thick and thin lines show respectively the median and interquartile values of the distribution. The median lines are accompanied by 1σ error limits estimated by bootstrap resampling and include the measured errors in $u - r$. Each bin contains 300 galaxies.

seen in the $\text{H}\alpha$ emission and SFR, confirming that the previous trends are not the result of aperture effects.

6 WHICH ASPECTS OF ENVIRONMENT DEFINE THE SF-DENSITY RELATION ?

To this point we have examined the environmental dependence on star-formation in galaxies using densities measured by smoothing over the nearest 5–10 galaxies. This has allowed us to describe the effects of the group and cluster environments on the galaxies. It is also possible that galaxies are affected by the presence of individual neighbouring galaxies, for example through disturbance from tidal forces.

In particular, we wish to reexamine for the much larger volume covered by the SDSS dataset the long noted morphological segregation of dwarf galaxies in the local ($\lesssim 30$ Mpc) neighbourhood, whereby dwarf ellipticals are confined to groups, clusters and satellites to massive galaxies, while dwarf irregulars tend to follow the overall large-scale structure without being bound to any of the massive galaxies (Binggeli, Tarenghi & Sandage 1990; Ferguson & Binggeli 1994). Einasto et al. (1974) first noted this segregation when comparing the spatial distribution of dwarf companions to our Galaxy and the nearby massive spirals M31, M81, and M101. He found a striking separation of the regions populated by dE and dIrr galaxies with dEs confined to being close satellites to the primary galaxies, and dIrr found at larger distances. In Paper I we found *no* isolated passively-evolving dwarf galaxy, always finding them gravitationally bound to clusters/groups or as satellites of $\gtrsim L^*$ field galax-

ies, differently from star-forming field dwarfs which appeared randomly distributed throughout the region.

In this context we wish to look at the effects of neighbouring galaxies on the star-formation histories of field galaxies ($\rho < 0.5$), i.e. those not in groups or clusters for which other processes may well dominate. There are two main physical mechanisms whereby a neighbouring galaxy could affect star-formation in another galaxy, tidal interactions, and ram-pressure stripping caused by the passage of the galaxy through the gaseous halo of its neighbour. In both of these mechanisms, the mass/luminosity of both the *central* galaxy (i.e. that which is being acted on) and the neighbouring galaxy are important for defining the strength of the effect on the *central* galaxy, in particular the greater mass-ratio between the neighbouring galaxy and the central galaxy, the stronger the effect is likely to be. To measure the effect of both the central and neighbouring galaxy masses, we split both the central and neighbouring galaxies into bins of luminosity. It is also important that we take out the effect of the large-scale ($\gtrsim 1$ Mpc) galaxy density from the equation, as galaxies in higher density regions will naturally have closer neighbours than lower density regions. To measure the effect of the presence of a neighbouring galaxy on the star-formation history of the central galaxy we compare the distances to the nearest neighbour (within a certain luminosity range) for passively-evolving and star-forming central galaxies that have the same mass/luminosity and the same large-scale environment (i.e. their local densities are the same). If the presence of a neighbouring galaxy is important for causing the central galaxy to become passive, we would expect passively-evolving central galaxies to have nearer neighbours (within a certain luminosity range) than star-forming galaxies of the same luminosity and large-scale environment.

In Figure 8 the distribution of distances between passively-evolving ($\text{EW}[\text{H}\alpha] < 2\text{\AA}$; red histograms) and star-forming ($\text{EW}[\text{H}\alpha] > 2\text{\AA}$; blue dashed histograms) central galaxies in field regions ($\rho < 0.5$) and their nearest neighbours are compared for both different magnitude ranges of central galaxies (in order of increasing luminosity from left to right as indicated) and different magnitude ranges of neighbouring galaxies (in order of increasing luminosity from top to bottom as indicated)

As a consequence of the SF-density relation, even in field regions passively-evolving galaxies will on average be in higher density regions than star-forming galaxies of the same luminosity, and hence on this basis alone would be expected to have closer neighbours on average. To remove this bias, we normalize the density distribution of the star-forming galaxies to that of the passively-evolving galaxies. This is done by splitting the galaxies into ten density bins of equal logarithmic width (0.2 dex) in the range $0.01 < \rho < 1$ and for each bin j identify a weight $\omega_j = N_{\text{passive}}^j / N_{\text{SF}}^j$ where N_{passive}^j and N_{SF}^j are the total number of passive and star-forming galaxies in that density bin. Each star-forming galaxy belonging to density bin j is then given the corresponding weight ω_j . The resulting weighted population of star-forming galaxies has the same density distribution as their passive counterparts. The blue-dashed histograms then represent the distribution of distances to the nearest neighbour for the star-forming galaxies where each galaxy i is represented by its corresponding weight ω_i .

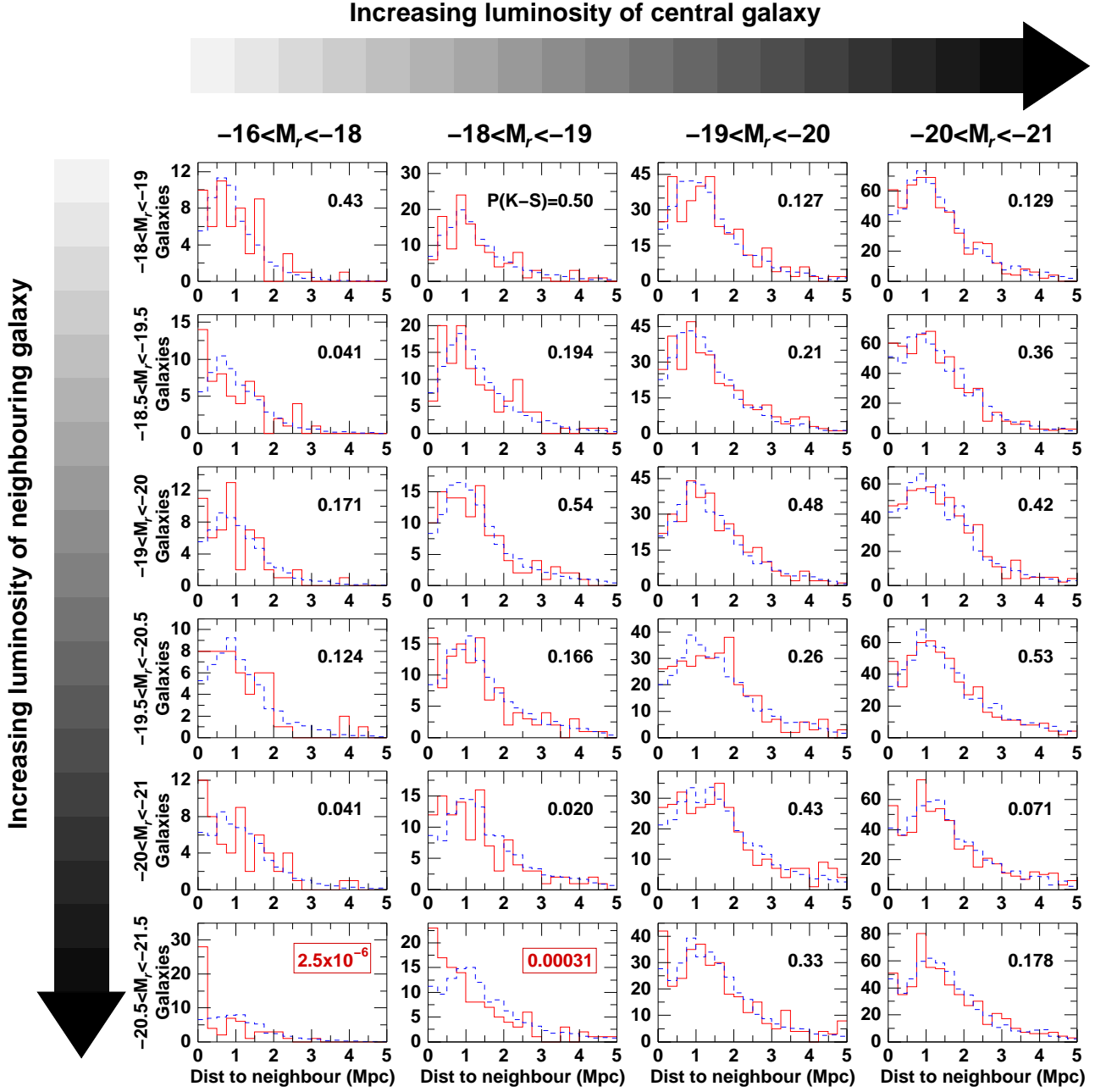


Figure 8. The distributions of distances to the nearest neighbouring galaxy within a specific luminosity range (in order of increasing luminosity from top to bottom as indicated) for $p < 0.5$ passive (red line) and star-forming (blue dashed line) *central* galaxies also within a specific luminosity range (in order of increasing luminosity from left to right as indicated). The probabilities that the two histograms are taken from the same distribution according to the Kolmogorov-Smirnov test are indicated in the top-right of each panel.

For each of the panels in Fig. 8 corresponding to a particular luminosity range for central and neighbouring galaxies, we estimate the significance of any differences between the distributions of the distance to the nearest neighbours of passive and star-forming galaxies (the red and blue histograms) using the Kolmogorov-Smirnov test. The results of these are indicated in the top-right of each panel, with significant differences ($P_{KS} < 0.01$) highlighted by red boxes.

Looking at the histograms in the last two columns (corresponding to central galaxies with $M_r < -19$) we see that the distributions of distances to the nearest neighbours

of any luminosity range are the same for the passively-evolving and star-forming galaxies. This implies that the star-formation histories of $M_r < -19$ galaxies are not significantly affected by the presence of individual galaxies in their immediate neighbourhoods, and instead it is only the global large-scale environment (as measured here by ρ) to which their SFRs are correlated. Equally if we look at the histograms in the top four rows (corresponding to neighbouring galaxies with $M_r > -20.5$) the distance distribution to the nearest neighbours are the same for passively-evolving and star-forming central galaxies of any luminosity range.

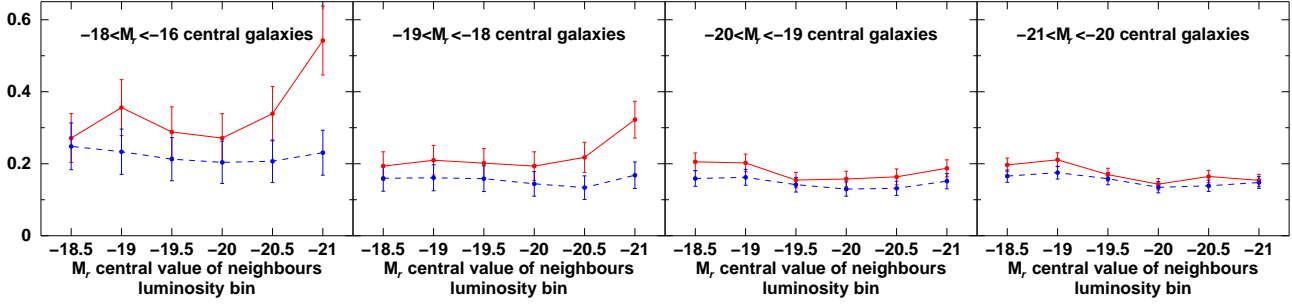


Figure 9. The fraction of passive (red lines) and star-forming (blue dashed lines) *central* galaxies which have within 0.5 Mpc one or more galaxies belonging to a fixed range of magnitude. Each panel corresponds to *central* galaxies within a specific magnitude range in order of increasing luminosity from left to right as indicated. The top left panel shows that dwarf passive field galaxies are much more likely to be found in the proximity of massive galaxies than star-forming dwarfs while the giant passive field galaxies show no preference as to their neighbours.

Hence star-formation in galaxies (at least for $M_r \lesssim -16$) is not significantly affected by the presence of neighbouring galaxies with $M_r \gtrsim -20$.

The only luminosity combinations of central and neighbouring galaxies that show any significant difference ($P_{KS} < 0.01$) between the distance distribution to the nearest neighbours of the passive and star-forming central galaxies are the two lower-left panels corresponding to low-luminosity central galaxies ($M_r > -19$) that have bright ($M_r < -20.5$) neighbours. In both these panels we see that passively-evolving dwarf galaxies ($M_r > -19$) are much more likely to have a nearby bright ($M_r < -20.5$) neighbour within ~ 500 kpc than would a star-forming galaxy of the same luminosity and having the same global environment (as measured with ρ). This implies that massive galaxies can influence the star-formation history of neighbouring dwarf galaxies, presumably orbiting as satellites, by causing them to become stop forming stars.

We reillustrate these effects in Figure 9 where we plot the fraction of *central* passive (red solid line) and star-forming (blue dashed line) galaxies that have one or more neighbours within 0.5 Mpc belonging to a fixed magnitude range. Each panel corresponds to a different magnitude range of central galaxies as before, while each point corresponds to one of the six magnitude ranges of neighbouring galaxies of Figure 8, the central value of which is indicated along the x-axis. The fractions of passive and star-forming giant ($-21 < M_r < -20$) galaxies with a neighbour within 0.5 Mpc are quite similar for every magnitude range of surrounding systems; not only, but the common fractions are quite constant independently of the luminosity of neighbouring galaxies. These observations show that both passive and star-forming massive galaxies have no preferences about their neighbours suggesting a uniform distribution for these systems. Different results are found for dwarf ($-18 < M_r < -16$) field galaxies. In fact, the fractions of passive dwarfs with neighbours within 0.5 Mpc are different from those found for their star-forming counterparts. The latter show a similar behavior with the field giants having, on average, no preference for neighbours of a particular luminosity. On the contrary the fraction of passive field dwarfs with a close-by galaxy strongly increases with the luminosity of the neighbour, underling that these systems, as was firstly pointed out by Einasto et al. (1974), are not uniformly dis-

tributed but are commonly found close to massive galaxies. This trend is also present, even if in a less strong way, for $-19 < M_r < -18$ *central* galaxies and disappears at brighter magnitudes.

These results suggest that the mechanisms transforming giants and dwarfs from star-forming to passive systems are different. The quite uniform spatial distribution of passive field giant galaxies underlines the negligible influence of any environmental interactions in stopping star-formation for these systems, while the frequent presence of nearby massive galaxies to passive field dwarf galaxies is a clear indication of the fundamental impact of massive galaxies on star-formation in nearby dwarf systems.

Out of the 252 passively-evolving dwarf galaxies in the lowest luminosity bin ($-18 < M_r < -16$) 48 are in regions with $\rho < 0.5$. Of these 48, 34 were found to have bright ($M_r < -20$) galaxies within ~ 500 kpc and ~ 500 km s $^{-1}$, 24 of which were within ~ 200 kpc and ~ 200 km s $^{-1}$. No further neighbours are identified if the magnitude limit is extended from $M_r < -20$ to $M_r < -19$. A further nine galaxies were identified as not actually being passively-evolving dwarfs, either having apparent H α emission not identified by the MPA/JHU pipeline, appearing blue, or having bad photometry which made the galaxy appear much fainter than it actually was.

Only five passively-evolving dwarf galaxies appear to be isolated, being 0.8–1.2 Mpc from the nearest bright galaxy. However, looking a little further out we find that all five appear to lie in the infall regions of galaxy groups at around 1.5–2 virial radii from the group centres, as indicated in Table 3. The centres and redshifts of each of the groups were identified as maxima in the luminosity-weighted galaxy density distribution, and the cluster velocity dispersions and virial radii determined as in Girardi et al. (1998) based on the galaxy radial velocities within 2 Mpc and $3\sigma_v$ of the cluster centre.

Although the first galaxy lies some 2.5 Mpc from MKW 8, this cluster is part of a larger structure which extends for ~ 7 Mpc around the “isolated” passive dwarf galaxy. It seems reasonable to assume this structure is still in the process of assembly, and hence the dwarf galaxy may have been left behind or thrown out by a previous interaction between the structures. The remaining nearby clusters are rather more isolated and regular, and so it seems less

RA, Dec (J2000)	z	M_r	d_{cl} (Mpc)	Group Name	Refs	N_{gal}	μ_{nu}	σ_z (km/s)	R_{vir} (Mpc)	T_X (keV)	$\log(L_X)$ (erg/s)
14:37:13.70, +02:28:35.9	0.0255	-17.67	2.56	MKW 8	1,2	147	0.0267	492	1.56	3.03	41.98
12:00:26.60, +01:40:07.6	0.0209	-17.32	1.46	MKW 4	1,2	99	0.0199	428	1.25	1.83	41.96
12:00:37.72, +02:08:47.9	0.0201	-17.61	1.41	MKW 4	1,2	99	0.0199	428	1.25	1.83	41.96
15:14:04.35, +03:24:04.9	0.0297	-17.82	0.76			6	0.0292	221	0.52		
09:47:15.48, +37:03:07.1	0.0223	-17.62	1.83	WBL 236	3,4	24	0.0219	324	0.96		41.76

References: (1) Rines & Diaferio (2006), (2) Popesso et al. (2004), (3) White et al. (1999), (4) Mahdavi & Geller (2004).

Table 3. Candidate isolated passively-evolving dwarfs and possible associated groups

likely that the other four dwarf galaxies were thrown out by cluster interactions. The most likely mechanism for these galaxies to have become passive is that in the past their orbits took them through their neighbouring group/cluster, whereupon they became passive through ram-pressure stripping and/or tidal interactions. From cosmological N-body simulations Mamon et al. (2004) find that infalling galaxies on radial orbits can bounce out of the clusters, reaching maximum clustercentric distances of between 1 and 2.5 virial radii. The main difficulty is to understand why these galaxies haven't been able to start forming stars again once they are no longer affected by the cluster environment. In particular, while these galaxies may have been completely stripped of gas while in the cluster, outside gas recycling from stellar mass loss should be able to produce enough gas to be detectable (e.g. Jungwiert, Combes & Palous 2001) and subsequently allow star-formation to restart after a few Gyr, although Grebel et al. (2003) suggest that ram-pressure from the passage of the galaxy through the low-density IGM may be sufficient to strip the stellar mass loss as it is recycled. It would be interesting to confirm whether these isolated dwarfs are truly passively-evolving or whether they have any detectable H I.

7 THE CONNECTION WITH AGN

In recent years observations have shown that at the heart of most if not all massive galaxies is a supermassive black hole (for a review see Ferrarese & Ford 2005), and it has become increasingly clear that the evolution of the galaxy and the central black hole are strongly interdependent. This is manifested most clearly by the tight correlations between the mass of the central supermassive black hole (SMBH) and the global properties of their host galaxies, such as the stellar mass of the bulge component ($M_{BH} = 0.0014 \pm 0.0004 M_{Bulge}$; Häring & Rix 2004), the stellar velocity dispersion (Gebhardt et al. 2000; Ferrarese & Ford 2005), and the host bulge Sersic index (Graham & Driver 2007). The scatter in the black hole masses around these relations are only of the order 0.3 dex.

Silk & Rees (1998) suggested that these correlations arise naturally through the self-regulated growth of SMBHs through accretion triggered by the merger of gas rich galaxies. Tidal torques produced by the merger channel large amounts of gas onto the central nucleus fuelling a powerful starburst and rapid black hole growth, until feedback from accretion is able to drive quasar winds and expel the remaining gas from the remnant galaxy. Hy-

drodynamical simulations of gas rich galaxy mergers incorporating star-formation, supernova feedback and black hole growth (Springel, di Matteo & Hernquist 2005a) confirm this picture, reproducing the observed $M_{BH} - \sigma$ relation (di Matteo, Springel & Hernquist 2005). Springel et al. (2005a) show that the presence of the central SMBH has a strong impact on the remnant galaxy, producing passively-evolving spheroidal galaxies (Springel et al. 2005b) consistent with the observed scaling relations (Robertson et al. 2006) and whose gas is heated by the quasar winds forming the observed X-ray emitting halos (Cox et al. 2006), whereas the remnant galaxies in models without SMBHs continued to form stars at a non-negligible rate.

Given the tight correlation between the mass of the central SMBH and that of the host galaxy, we should expect the effects of AGN feedback to be strongly dependent on galaxy mass, being reduced or even negligible for low-mass galaxies. Springel et al. (2005b) find that for merging galaxies with $\sigma = 80 \text{ km s}^{-1}$ the effects of black hole growth on the remnant are negligible, the spheroids that form remaining gas rich with ongoing star-formation. Indeed in low-mass galaxies SMBHs may not form at all during mergers. The rapidity of the gas accretion onto the central object depends on the depth of the potential well of the host galaxy, and in low-mass galaxies the accreting gas may have time to fragment and form stars, preventing further dissipation and collapse of the gas (Haehnelt, Natarajan & Rees 1998). Indeed most (50–80%) dwarf galaxies ($M_B \gtrsim -18$) appear to host central compact stellar nuclei, regardless of their morphological class (Côté et al. 2006; Rossa et al. 2006), the masses of which scale with the mass of their host galaxy, following the same correlation as that observed for SMBHs (Ferrarese et al. 2006; Wehner & Harris 2006).

In recent years there have been significant advances in the theoretical framework in understanding galaxy evolution, in particular the ability of semi-analytic models to reproduce the global properties observed in the current large scale surveys such as the SDSS. One large problem that the theoreticians have been facing is reproducing the observed break and exponential cut off in the luminosity function at the bright end along with the observation that most massive galaxies are passively-evolving, and have been for many Gyr. These massive galaxies have halos of X-ray emitting hot gas, which without constant energy injection should cool through radiative losses onto the galaxy, fuelling further star-formation (Mathews & Brighenti 2003). However, no evidence of this cooling gas is observed, and AGN feedback has often been put forward as a means of supplying energy to the hot gas, and preventing it from cooling.

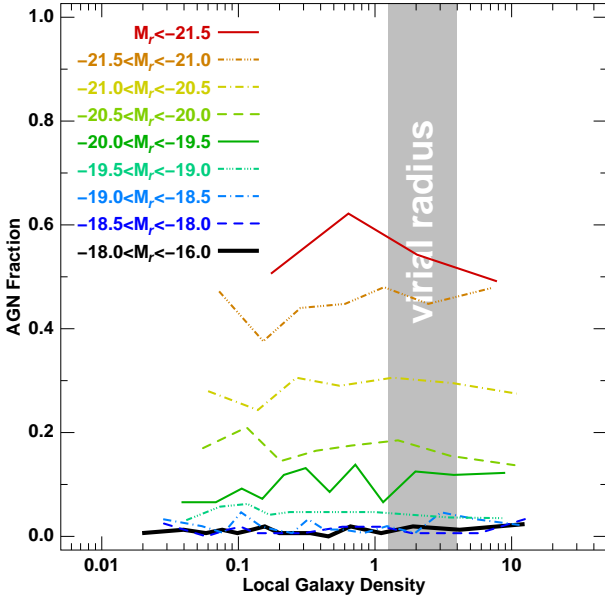


Figure 10. The fraction of galaxies classed as AGN from their emission line ratios as a function of local density. Each coloured curve corresponds to a different luminosity bin as indicated. Each density bin contains 150 galaxies.

Croton et al. (2006) have developed semi-analytic models which include AGN feedback to prevent this gas cooling onto massive galaxies, which have been able to successfully reproduce the exponential cut-off in the bright end of the luminosity function and the fact that most massive galaxies are quiescent and dominated by old stars. It is important to note that the feedback considered here is low-level AGN activity from the quasi-continuous accretion from a static atmosphere of hot gas that is in thermal equilibrium with the DM halo.

To examine the possible role of AGN feedback in terminating star-formation in galaxies Fig. 10 shows how the AGN fraction depends on both luminosity and environment. Each coloured curve shows the fraction of galaxies classed as AGN from their location in the $[\text{NII}]\lambda 6584 / \text{H}\alpha$ versus $[\text{OIII}]\lambda 5007 / \text{H}\beta$ diagnostic diagram (Baldwin et al. 1981) as a function of local density for a particular luminosity range as indicated. We note that these diagnostics are not sensitive to type 1 AGN with broad-line emission, however these are mostly limited to massive galaxy hosts and at these redshifts they constitute only $\lesssim 1\%$ of the $M_r \lesssim -20$ galaxy population (e.g. Hao et al. 2005; Sorrentino et al. 2006). For ease of comparison, the colours and curves correspond to the same luminosity ranges as Fig. 3.

The fraction of galaxies with an AGN remains constant with local density from the cores of clusters to the rarefied field, for each of the luminosity ranges covered. This is consistent with the result obtained by Miller et al. (2003) for bright ($M_r < -20$) galaxies. Whereas the AGN fraction is independent of density, it varies by more than an order of magnitude with the galaxy’s luminosity, from $\sim 50\%$ for the brightest galaxies ($M_r < -21$) to 0–3% by $M_r \sim -18$ (see also Kauffmann et al. 2003c). Hence, the processes that power an AGN must be internal to the galaxy and dependent only on the mass/luminosity of

the galaxy, while the galaxy’s local environment has little or no effect on its ability to host or power an AGN. Most of the AGN detected here are low-luminosity AGN powered by low-level, quasi-continuous accretion of gas onto a SMBH. High-luminosity ($L[\text{OIII}] > 10^7 L_\odot$) AGN and quasars are instead preferentially found in the outskirts of clusters or in low-density regions, being relatively absent in cluster cores (Kauffmann et al. 2004; Söchting et al. 2004; Ruderman & Ebeling 2005). These results are consistent with the model for high-luminosity AGN/quasars being triggered by the merging of two gas-rich galaxies, as in the centres of clusters most galaxies have already lost most of their gas.

Martini et al. (2006) find that only $\sim 10\%$ of their X-ray selected AGN in clusters had obvious optical spectroscopic AGN signatures, although in total they found only 5% of $M_r < -20$ cluster members had X-ray emission characteristic of AGN, which is much smaller than the $\sim 30\%$ of $M_r < -20$ galaxies observed here with the optical signatures of AGN. These optically dull AGN are found to have higher inclination angles than those showing optical emission, indicating that extranuclear dust in the host galaxy hides the emission lines of optically dull AGN (Rigby et al. 2006). It should be noted that AGN detection rates are subject to strong aperture biases, because as the physical aperture subtended by the SDSS fibre becomes larger, the nuclear emission from the AGN is increasingly diluted by emission from the surrounding host galaxy. This effect is particularly great for low-luminosity AGN and LINERs where the fraction detected in massive galaxies from their SDSS spectra drops from $\sim 60\%$ to $\sim 20\%$ with increasing redshift (Kauffmann et al. 2003a; Kewley et al. 2006). For our sample, being at low redshifts the SDSS fibres cover only the nuclear region ($\lesssim 1\text{kpc}$) of massive galaxies and so we should not lose a significant fraction of AGN due to dilution of their emission. Another possible bias to the results presented here could be signal-to-noise effects in the classification of AGN. In particular, a 3σ detection of $\text{H}\alpha$ emission is required, yet the median $\text{H}\alpha$ equivalent width of galaxies classed as AGN is just 1.56 \AA . This could produce a dependency on the r -band magnitude of the galaxy, as the median uncertainty in $\text{EW}(\text{H}\alpha)$ rises from 0.1 \AA at $r = 14$ to 0.5 \AA by $r = 17.77$. Thus a significant fraction of faint galaxies ($r \gtrsim 17$) may not be classified as AGN simply due to their low signal-to-noise spectra. However, although this could produce in theory a small bias against detecting AGN in the dwarf galaxies, it should be negligible in comparison to the observed trend with luminosity presented in Fig. 10.

The most striking result in Fig. 10 is the lack of AGN in dwarf galaxies. As shown in Fig. 3 these galaxies are star-forming and many have strong emission lines due to this star-formation, which could in theory affect the ability to detect any low-luminosity AGN from the BPT diagnostic method. However, as Kauffmann et al. (2003c) show that the presence of even a low-luminosity AGN with $10^5 < L[\text{OIII}] < 10^6 L_\odot$ would perturb the emission-line ratios enough to be detected in 93% of dwarf galaxies classified as star-forming.

Although the biases due to signal-to-noise effects, dust-obscuration, aperture effects, emission from star-forming regions etc are likely to affect the ability to detect AGN in galaxies, the observed trend with luminosity is very strong,

and appear broadly consistent with expectations from the tight correlation between the mass of the central SMBH and the host bulge component. At the lowest luminosities, the predicted mass of the central black hole (if there is one at all) is too low to be able to power an AGN detectable in the optical spectrum. With increasing galaxy luminosity, the typical mass of the central SMBH increases (Ferrarese & Ford 2005), becoming increasingly capable of powering an AGN detectable in the optical spectrum, resulting in the AGN fraction increasing with luminosity.

A comparison between Figs. 3 and 10 finds a remarkable match between the fraction of passive galaxies in low-density environments and the AGN fraction for all of the luminosity bins covered. In these regions, environment-related processes such as galaxy harassment or ram-pressure stripping are not effective, and their star-formation histories are dependent only on mechanisms *internal* to the galaxy, such as their merger history and feedback processes. The strong correlation between the fraction of AGN and passive galaxies in these regions suggests a direct connection, with galaxies becoming passive through AGN feedback, and appears consistent with the current model of the coevolution of AGN and galaxies (e.g. Springel et al. 2005a; Hopkins et al. 2006a,b, 2007b).

8 COMPARISON WITH SEMI-ANALYTIC MODELS

To better understand the physical mechanisms that contribute to the observed different environmental trends of galaxies with luminosity, we compare our results with those produced by the semi-analytic models of Croton et al. (2006, hereafter C06). These are implemented on top of the Millennium Run N-body simulation, currently the largest dark matter simulation of the concordance Λ CDM cosmology with $\sim 10^{10}$ particles in a periodic box $500h^{-1}$ Mpc on a side, giving a mass resolution of $8.6 \times 10^8 h^{-1}$ Mpc (Springel et al. 2005c). Dark matter halos and subhalos are identified as having 20 or more bound particles, their merging trees constructed, which are subsequently used to populate the halos and subhalos with galaxies according to the prescriptions described in C06. For each galaxy there are four components: stars, cold gas in the disk, hot gas in the halo, and the central supermassive black hole. The two novel features of the C06 model are: (i) the modeling of gas infall from the halo onto the cold disk, which occurs either through rapid cooling primarily in low-mass galaxies, or cooling from a static halo of hot gas heated by accretion shocks, the dominant process in massive galaxies; and (ii) its inclusion of the growth of black holes, and their subsequent effects on the cold and halo gas in the galaxy. These effects are two-fold, during galaxy mergers a certain fraction of the cold gas is accreted by the black hole, although any resultant energy released such as quasar winds are not modeled, while instead low-level accretion of the hot gas in the halo on the black hole is also described and results in energetic ‘radio mode’ feedback which can prevent the further cooling of gas from the halo.

As described in Appendix A the resultant galaxy properties are used to create a mock SDSS redshift catalogue, and the local density for each galaxy estimated in the same

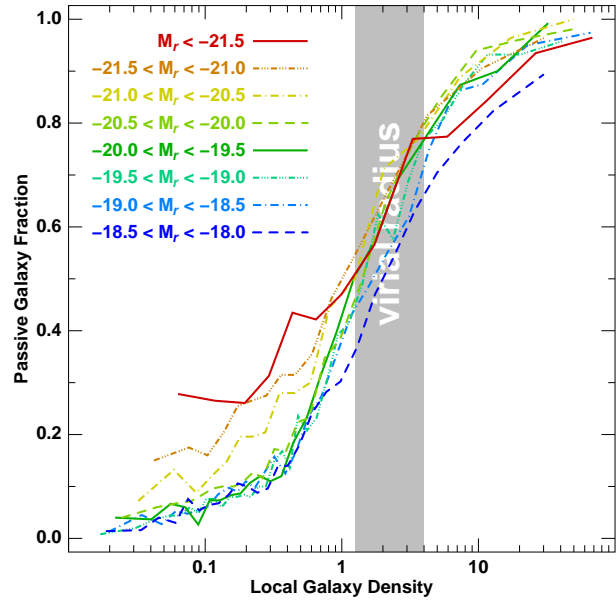


Figure 11. The fraction of passively-evolving galaxies as a function of local density in the C06 semi-analytic model. Each coloured curve corresponds to a different luminosity bin as indicated and are analogous to those in Fig. 3. Each density bin contains 150 galaxies.

manner. As in the mock catalogues we do not have information regarding the $H\alpha$ emission from each galaxy, we instead define galaxies as being passive if they are both red ($u - r > 2.2$) and have a current specific star-formation rate (SFR/M) less than 10% that of the median value of star-forming galaxies ($\sim 10^{-10} h^{-1} M_{\odot} \text{yr}^{-1} / M_{\odot}$).

Figure 11 shows the resultant fraction of passively-evolving galaxies as a function of both local density and luminosity. Each coloured curve corresponds to a different luminosity bin as indicated, and are analogous to those for the SDSS dataset shown in Fig. 3 allowing a direct comparison. There are several important discrepancies between the model predictions and the SDSS data, which indicate areas where the models do not accurately describe the physical processes which define whether galaxies are still forming stars or not.

The most notable difference is that the much smaller apparent luminosity dependence in the fractions of passively-evolving galaxies in low-density regions from the C06 models in comparison to those observed in the SDSS data. Whereas the passive galaxy fraction increases from $\sim 2-8\%$ to $\sim 30\%$ from the lowest to the highest luminosity bins in the models, in the SDSS dataset the increase over the same luminosity range is from 0% to $\sim 50\%$. As in these low-density regions environmental processes should not be important, the differences must be due to the models treatment of internal feedback processes that truncate and regulate star-formation in galaxies. The discrepancies appear greatest for the most massive galaxies where AGN feedback should be the most important mechanism for truncating star-formation in galaxies, and so this suggests that the prescription for AGN feedback in the C06 model is not efficient enough, the most likely cause of this being the neglect of feedback from quasar winds.

There is also a discrepancy at the low-luminosity end, with fewer passively-evolving dwarf galaxies observed than predicted by the models. While in the SDSS data the passive galaxy fraction continues to fall with luminosity until it reaches zero at $M_r \sim -18$, in the models there appears no luminosity dependence for galaxies fainter than $M_r \gtrsim -20.5$, in any environment. The C06 model predicts that $6.1 \pm 0.3\%$ of $-18 < M_r < -19$ galaxies in field regions ($\rho < 0.2$) should be passively-evolving, a factor ~ 3 greater than the $1.9 \pm 0.3\%$ observed in the SDSS dataset. Three-quarters of these galaxies in the C06 model are satellites to $M_r < -20$ galaxies, indicating that this excess most likely related to how the C06 model deals with the evolution of satellite galaxies. In the C06 model, as in most semi-analytic models, when a galaxy becomes a satellite within a more massive halo, it instantly loses the gas from its halo to that of its host, “suffocating the galaxy”, and consequently uses up the remainder of its cold gas until it is no longer able to continue forming stars (Larson et al. 1980). This finding of too many passively-evolving dwarf galaxies in low-density environments suggests that the incorporation of “suffocation” into the model is too efficient, terminating star-formation in galaxies too rapidly once they become satellites. This is confirmed by Weinmann et al. (2006b) who split galaxies in the SDSS and C06 catalogues into satellite and central galaxies, and find that in the C06 model catalogues just $\sim 20\%$ $M_r \sim -18$ satellite galaxies are blue, much lower than the $\sim 60\%$ observed in the SDSS data.

Bekki, Couch & Shioya (2001, 2002) performed N-body and hydrodynamical simulations following the effects of the cluster environment on the gaseous halo of an infalling L^* spiral galaxy, and found that for a cluster of mass $\sim 10^{14} M_\odot$ the combination of the cluster tidal field and ram-pressure were able to efficiently strip $\sim 80\%$ of the halo gas over a period of 1–2 Gyr. The stripping should be more rapid for lower mass galaxies. Balogh, Navarro & Morris (2000) elaborated the model of Larson et al. (1980), indicating that the gradual decline of star-formation on the ~ 3 Gyr timescales predicted by suffocation could reproduce the Butcher-Oemler effect and the observed gradual star-formation density relations extending well beyond the cluster virial radius (e.g. Lewis et al. 2002; Treu et al. 2003). By simply assuming the Schmidt-Kennicutt law, Balogh et al. (2000) obtain a relation for the decline in star-formation where no further gas accretion is possible as,

$$\text{SFR}(t) = \text{SFR}(0) \left(1 + 0.33 \frac{t}{t_e}\right)^{-3.5} M_\odot \text{ yr}^{-1}, \quad (3)$$

where $\text{SFR}(0)$ is the initial star-formation rate, and $t_e \approx 2.2 [\text{SFR}(0)/M_\odot \text{ yr}^{-1}]^{-0.29}$ Gyr is the characteristic gas consumption time-scale, including the effects of gas recycling. For a typical L^* spiral galaxy with $\text{SFR}(0) \sim 5 M_\odot \text{ yr}^{-1}$ we obtain $t_e \sim 1.4$ Gyr, resulting in the galaxy taking ~ 4 Gyr to become passive ($\text{SFR}(t)/\text{SFR}(0) \sim 0.1$), a time-scale consistent with the cluster spiral population in $z \sim 0.4$ clusters becoming passive by $z = 0$.

Applying Eq. 3 instead to a typical field dwarf galaxy with $M_r \sim -18$ and $\text{SFR}(0) \sim 0.2 M_\odot \text{ yr}^{-1}$ we obtain $t_e \sim 3.5$ Gyr, resulting in the galaxy taking ~ 10 Gyr to become passive, consistent with their observed gas depletion time-scales of ~ 20 Gyr (van Zee 2001). Hence, even if deprived of further gas accretion through suffocation, star-

formation in dwarf galaxies occurs at a sufficiently low rate that they are unlikely to have consumed all their gas and become passive by the present day if they are acted on only by the mild stripping envisaged in suffocation.

If suffocation alone is unable to terminate star-formation in the dwarf satellites of massive galaxies, then a stronger form of gas stripping is required. Mayer et al. (2001, 2006) show that dwarf spiral galaxies orbiting a Milky Way type galaxy can suffer significant mass loss and have their entire gas content removed or used up in a star-burst, transforming them into passive dwarf ellipticals over a period of ~ 5 Gyr through the combination of tidal shocks and ram-pressure stripping if their orbits take them within ~ 50 kpc of the primary. Such behaviour is difficult to model within a cosmological simulation such as that of C06, in particular as the tidal forces acting on the dwarf satellites change rapidly along their orbits, such that the star-formation histories and evolutions (in terms of mass loss) of dwarf satellites could be very strongly affected by even small variations in their orbits (Kravtsov, Gnedin & Klypin 2004; Sales et al. 2007).

Looking at the possible effect of the Millenium simulation neglecting tidal stripping on the satellite population, we find an overabundance of faint satellite galaxies around massive field galaxies in the models in comparison to the SDSS data. In particular for each $M_r < -20$ field galaxy we observe on average 0.125 ± 0.007 $-19 < M_r < -18$ galaxies that lie within 250 kpc and 500 km s^{-1} of it (i.e. that are probable satellites), whereas in the C06 model we find on average 0.195 ± 0.004 . A certain fraction of these galaxies will in fact be interlopers, and should be subtracted from this analysis. We estimate the number of interlopers as the number of dwarf ($-19 < M_r < -18$) galaxies found around a dwarf galaxy which has no $M_r < -20$ galaxy within 1 Mpc and 1000 km s^{-1} , so that neither of the dwarf galaxies are satellites, obtaining a value of 0.083 ± 0.003 per galaxy. This takes into account the natural clustering of dwarf galaxies, independent of the presence of nearby giant galaxies. An alternate estimate for the number of interlopers can be made by assuming interlopers are distributed evenly over the volume covered, and so in this case we would expect 0.019 dwarf galaxies within the volume around each $M_r < -20$ galaxy. Considering the contamination from interlopers to be between these two values, we estimate the excess dwarf satellites in the Millennium simulation to be 65–167%.

9 DISCUSSION

Using a volume-limited sample of galaxies from the SDSS DR4 spectroscopic dataset we have examined the star-formation activity of galaxies as a function of both luminosity and environment, the main results of which are summarized in Figure 3. In high-density regions the bulk of galaxies are passively-evolving independent of mass. Many processes could contribute to terminating the star-formation in these galaxies, either internal to the galaxy or related to the hostile cluster environment, making it difficult to identify those which are most important. To gain insights into the relative importance of these different mechanisms we instead focus on galaxies in low-density regions for which we can be sure that their star-formation histories have not been influenced

by cluster-related processes (thanks to our robust separation of cluster and field populations). Hence the star-formation histories of these galaxies can only be influenced by internal mechanisms such as merging, gas consumption through star-formation and AGN feedback.

We find that the fraction of passively-evolving galaxies in field regions drops steadily from $\sim 50\%$ at $M_r \lesssim -21$ to zero by $M_r \sim -18$. This implies that internal mechanisms are not responsible for the formation of passively-evolving dwarf galaxies, while they become increasingly important with galaxy mass for driving their star-formation histories. This would be consistent with the increasingly early and rapid conversion of gas into stars for more massive galaxies resulting from the Kennicutt-Schmidt law ($\Sigma_{SFR} \propto \Sigma_{gas}^{1.4 \pm 0.1}$; Kennicutt 1998; Schmidt 1959), which has been shown to hold over several orders of magnitude of gas density, in conjunction with the appearance of a critical gas density below which star-formation does not occur (Martin & Kennicutt 2001). Hydrodynamical simulations of the formation of massive $\sim M^*$ field galaxies show that passively-evolving elliptical galaxies can be produced without recourse to major mergers or feedback mechanisms consuming their gas in a short burst ($\lesssim 2$ Gyr) of star-formation at $z \gtrsim 2$ (Chiosi & Cararro 2002; Naab et al. 2007). In dwarf galaxies instead star-formation occurs very inefficiently resulting in gas consumption time-scales much longer than the age of the Universe (van Zee 2001) and global star-formation rates that have remained approximately constant since $z \sim 3$ (Panter et al. 2007). These simulations and the observed studies of the global decline of star-formation since $z \sim 1$ through downsizing (Heavens et al. 2004; Noeske et al. 2007a,b) suggest that gas exhaustion through star-formation may play a dominant role in the *global* evolution of star-formation.

This does not appear to be the complete answer, in particular it does not explain the wide variety of star-formation histories seen in field $\sim M^*$ galaxies (Haines et al. 2006b), where completely interspersed mixtures of young and old galaxies (in terms of their stellar populations) are found. This instead suggests that some stochastic processes play a role in determining the star-formation histories of massive galaxies, the most natural being their hierarchical assembly through mergers and the resultant growth of SMBHs and subsequent AGN feedback effects (Hopkins et al. 2006a,b, 2007b). Moreover we find a close mirroring of the increase in AGN fraction with galaxy luminosity to that observed for the passive galaxies in field regions, suggesting a direct connection between nuclear activity and galaxies becoming passive, reflecting the increasing importance of AGN feedback with galaxy mass for their evolution.

9.1 Massive galaxies affected by merging

In the case of massive galaxies ($\mathcal{M} \gtrsim 10^{10.3} M_\odot$; $M_r \lesssim -20$) we confirm the recent results on the environmental dependence of star-formation (Lewis et al. 2002; Gómez et al. 2003; Tanaka et al. 2004; Rines et al. 2005), finding gradual trends for the fraction of passively-evolving bright galaxies with environment that extend to the lowest densities studied (§ 4). Furthermore we find that this correlation with the local density is independent of the presence or absence of *individual* neighbouring galaxies (§6). Rines et al. (2005)

find that the fraction of passively-evolving galaxies depends on the local density, and this dependency is the same for galaxies in different types of global environment (within the cluster virial radius, in infall regions, and the field), while Tanaka et al. (2004) find no dependence on system richness for galaxies residing in groups with $\sigma > 200 \text{ km s}^{-1}$. In Section 5 we also find that the distribution of EW(H α) of massive galaxies with *current* star-formation shows no dependence on local density in agreement with the results obtained by Balogh et al. (2004a), Tanaka et al. (2004) and Rines et al. (2005). These results together indicate a limited role for mechanisms specific to cluster environments on the termination of star-formation in massive galaxies, in particular excluding mechanisms which result in a gradual decline in the SFR of infalling galaxies. Instead star-formation in massive galaxies is terminated rapidly (on time-scales $\lesssim 1$ Gyr) through processes that depend only marginally on the local density and/or occur at high-redshifts such that ongoing transformations are rare.

This early cessation of star-formation in massive passively-evolving galaxies and the independence of the star-formation histories on the global cluster environment, point towards the evolution of massive galaxies being driven primarily by *internal* mechanisms and their merger history (Hopkins et al. 2007b). The environmental trends are then defined by the initial conditions in which galaxies form, whereby massive galaxies are formed earlier preferentially in the highest overdensities in the primordial density field (Maulbetsch et al. 2007), and have a more active merger history (Gottlöber et al. 2001), than those that form in the smoother low-density regions. This implies the environmental trends should be imprinted early on in the massive galaxy population, as is observed with the morphology–density and colour–density relations being already largely in place by $z \sim 1$ (Smith et al. 2005; Cooper et al. 2006), and possibly apparent even at $z > 2$ (Quadri et al. 2007).

This rapid formation of massive galaxies and the early shutdown of star-formation is produced naturally in the monolithic collapse model, where the deep potential wells allow for rapid and efficient conversion of the gas into stars according to the Kennicutt-Schmidt law (Chiosi & Cararro 2002) in a short burst ($\lesssim 2$ Gyr) of star-formation at $z \gtrsim 2$.

While the monolithic collapse model appears at odds with the hierarchical growth of structures produced in Λ CDM models, Merlin & Chiosi (2006) are able to reproduce the same qualitative star-formation histories for massive galaxies within a hierarchical cosmological context, most of the merging of substructures occurring early in the galaxy life ($z > 2$). This so-called “revised monolithic” scheme is consistent with the observed rapid evolution and growth of massive galaxies through merging at $z > 1$ (Conselice 2006), and the mild evolution in the number density of massive ($\mathcal{M} \gtrsim 10^{10.5} M_\odot$) red galaxies to $z \sim 1$ (Bell et al. 2004; Willmer et al. 2006) and beyond (Glazebrook et al. 2004; Cirasuolo et al. 2006; Renzini 2006). Equally the observed bimodality in the colour distribution of galaxies at $z \sim 1.2$ (Bell et al. 2004; Willmer et al. 2006) implies that star-formation must be truncated rapidly and completely in massive galaxies at $z \gtrsim 1.5$ or even earlier (Kriek et al. 2006). Given the short gas-consumption time-scales of massive galaxies, to maintain star-formation to the present day would require massive galaxies to con-

tinuously accrete of fresh gas from their surroundings (Larson et al. 1980). However, massive galaxies in halos of mass $\gtrsim 6 \times 10^{11} M_{\odot}$ stable virial shocks form which heat infalling gas to the virial temperature, significantly reducing the accretion rate onto the galaxy, and making the gas vulnerable to feedback effects such as AGN (Dekel & Birnboim 2006). Indeed in many massive galaxies further accretion of gas may be completely shutdown, resulting in the subsequent termination of star-formation without the need for further quenching mechanisms such as mergers or AGN feedback (Birnboim, Dekel & Neistein 2007).

In Section 7 we determined the fraction of galaxies with optical AGN signatures as a function of both luminosity and environment. We find the AGN fraction to be independent of local density for galaxies of a given luminosity for $M_r < -18$. In contrast the AGN fraction is strongly luminosity dependent, increasing from $\sim 0\%$ at $M_r \sim -18$ to $\sim 50\%$ by $M_r \sim -21$ in a way that closely mirrors the luminosity-dependence of the passive galaxy fraction in low-density environments. These results suggest that the ability of a galaxy to host an AGN depends only on its mass, as would be expected from the tight $M_{\text{BH}} - \sigma$ relation (Ferrarese & Ford 2005), while the strong correlation between the fractions of galaxies hosting AGN and being passive suggests a direct connection between nuclear activity and a galaxy becoming passive. This appears consistent with the current models of the coevolution of AGN and galaxies (e.g. Springel et al. 2005a; Hopkins et al. 2006a,b, 2007b), and reflects the increasing importance of AGN feedback with galaxy mass for their evolution, and its increasing efficiency in permanently shutting down star-formation, by expelling gas from the galaxy through quasar winds (di Matteo et al. 2005) and/or preventing further cooling of gas from the surrounding halo (Croton et al. 2006).

It seems impossible for environmental processes to be able to shut off star-formation in massive galaxies at such an early epoch as required: ram-pressure stripping for example is unlikely to be efficient until later epochs ($z \lesssim 1$) once the dense cluster ICM has had time to build up (Kapferer et al. 2007), while both galaxy harassment and suffocation take several Gyr to terminate star-formation in galaxies, and simply haven't had time to act. Moreover, even in field regions where these processes are not efficient, massive, passively-evolving galaxies are seen to be in place at $z > 1$, with only slight differences are observed in the mean stellar ages and mass-to-light ratios of galaxies in diverse environments (Thomas et al. 2005; Smith et al. 2006; van Dokkum & van der Marel 2007).

Although the formation of passively-evolving early-type galaxies through merging largely took place at $z \gtrsim 1$, there is evidence indicating this process is continuing at lower redshifts. Early-type galaxies that are currently passively-evolving, but with remnant young (1–4 Gyr) stellar populations or E+A spectra indicating < 1 Gyr old stars, are preferentially located in low-density environments or poor groups, where low-velocity interactions should be most frequent (Goto 2005; Nolan, Raychaudhury, & Kabán 2007). The fraction of blue, spiral galaxies in clusters is also observed to drop rapidly from $z \sim 0.5$ to $z \sim 0$ — the Butcher-Oemler effect — while many spiral galaxies in local clusters show strong evidence of being transformed now by ram-pressure

stripping (e.g. Solanes et al. 2001; Koopmann & Kenney 2004; van Gorkom 2004).

As discussed in § 8 the mechanism of suffocation was proposed by Larson et al. (1980) to explain the Butcher-Oemler effect, by stripping the extended gas reservoirs of recently accreted spiral galaxies in clusters at $z \sim 0.4$, slowly transforming them by the present day into passively-evolving galaxies by exhausting their remaining gas supplies through star-formation. However, suffocation should not change the morphology or radial profiles of the spiral galaxies, turning them into anemic spirals (van den Bergh 1976) rather than the S0s whose numbers in clusters have increased rapidly since $z \sim 0.4$ mirroring the decline of cluster spirals (Dressler et al. 1997; Desai et al. 2007).

Instead, studies of spiral galaxies in the Virgo cluster find that a much larger fraction of them have truncated H α and H I radial profiles (52%) than appear simply anemic (6–13%) with globally reduced star-formation and gas densities (Koopmann & Kenney 2004). Similarly, Vogt et al. (2004) find a significant fraction of spirals with asymmetric H α profiles and H I rotation curves in nearby rich clusters. It is difficult for suffocation to produce these truncated or asymmetric H α and H I profiles, and instead it appears more likely that a process such as ram-pressure stripping actively removes the gas from the outside-in, and Boselli et al. (2006) show that ram-pressure stripping is able to reproduce the observed radial profiles. This outside-in removal of the gas should also produce inverted colour gradients in which the inner regions of the galaxy are bluer than the outer regions, as star-formation is truncated earlier in the periphery than the core of the galaxy, an effect which has been observed for the Virgo spiral NGC 4569 (Boselli et al. 2006).

These truncated spiral galaxies are mostly confined to the inner 1–1.5 Mpc of the Virgo cluster, that is within the virial radius, although there are some well outside the virial radius (Koopmann & Kenney 2004). All of the asymmetric spiral galaxies are located within $1 h^{-1}$ Mpc of the cluster centres with the truncation of the H I and H α emission preferentially along the leading edge (Vogt et al. 2004). These results are more consistent with the effects of ram-pressure stripping which should only affect massive galaxies within the cluster cores ($\lesssim 0.3 R_{\text{vir}}$; Roediger & Hensler 2005), although as the H I deficient spiral galaxies are observed to be on highly-elliptical radial orbits (Solanes et al. 2001), those truncated or asymmetric galaxies at $0.3 \lesssim (r/R_{\text{vir}}) \lesssim 1.5$ could have recently passed through the cluster core (Mamon et al. 2004).

The few anemic spirals with globally reduced H α and H I emission are generally found further from the cluster centres than truncated galaxies, half of them are outside the virial radius (Koopmann & Kenney 2004), while Goto et al. (2003) find that passive spirals in the SDSS are generally found in the outskirts of clusters at $1\text{--}10 R_{\text{vir}}$. It could then be that these galaxies are the natural results of suffocation, and may represent an early phase of evolution from spirals to passively-evolving S0s. The finding of significant numbers of truncated spiral galaxies in clusters, implies that the complete removal of gas and transformation into passively-evolving galaxies does not occur rapidly, at least in Virgo-like clusters. This appears inconsistent with our finding of no environmental dependence in the H α emission of bright star-forming galaxies, as that implies the transformation is

either rapid or occurs at high-redshift. One plausible explanation could be due to our measuring the H α emission from a confined region in the galaxy centre rather than the entire disk, and that star-formation within the truncation radius is relatively unaffected, until the galaxy orbit brings it sufficiently close to the cluster centre that the remaining gas is completely stripped, rapidly terminating star-formation across the galaxy.

9.2 Dwarf galaxies affected by their environment

In Section 4 we showed that the make-up of the dwarf galaxy population varies strongly with environment. Whereas in galaxy groups and clusters the bulk of dwarf galaxies are passively-evolving, as the local density decreases the fraction of passively-evolving dwarfs drops rapidly, reaching zero in the rarefied field. Indeed for the lowest luminosity range covered ($-18 < M_r < -16$) none of the ~ 600 galaxies in the lowest density quartile are passively-evolving. In Section 6 we examined in detail the immediate environment of those few passively-evolving dwarf galaxies in field regions, finding them very strongly clustered around bright ($M_r \lesssim -20.5$) galaxies. Almost without exception those passively-evolving galaxies outside groups and clusters appear to be satellites bound to massive galaxies.

This association of passively-evolving dwarf galaxies as satellites within more massive halos is consistent with the analysis of Zehavi et al. (2005) of the dependence of the galaxy two-point correlation function on luminosity and colour. They find that whereas the overall amplitude of clustering decreases monotonically with magnitude over $-23 \lesssim M_r \lesssim -18$, the clustering of *red* galaxies on $\lesssim 1$ Mpc scales is strongest for $M_r > -19$. They are able to describe these results using halo occupation distribution (HOD) models in which the faint red galaxies are nearly all satellites in high-mass halos.

These results confirm and significantly extend the long noted morphological segregation of dwarf galaxies in the local ($\lesssim 30$ Mpc) neighbourhood, with dwarf ellipticals (dEs) confined to groups, clusters and satellites to massive galaxies, while dwarf irregulars (dIrrs) tends to follow the overall large-scale structure without being bound to any of the massive galaxies (Einasto et al. 1974; Ferguson & Binggeli 1994). Here dwarf ellipticals (dEs) are generally defined as galaxies with $-18 \lesssim M_B \lesssim -14$ having smooth, symmetrical surface-brightness profiles implying no spiral structures or star-forming regions, and typically have very low H I mass fractions, and hence we identify these galaxies with our passively-evolving dwarf galaxies, although there are galaxies (e.g. NGC 205 which are classed as dEs but have recent star-formation in their central regions; Mateo 1998).

The morphological segregation of dwarf galaxies was first noted by Einasto et al. (1974) who compared the spatial distributions of dwarf companions to our Galaxy and the nearby massive spirals M 31, M 81 and M 101. They found a striking separation of the regions populated by dE and dIrr galaxies with a well defined line of segregation which had a strong luminosity dependence, with more luminous dEs constrained to smaller regions around the primary galaxy. They argued that tidal effects would be insufficient to produce this segregation and that a dense corona of halo gas around massive galaxies is necessary to strip

the gas from the satellites as they move through the corona (Gunn & Gott 1972). In the Local Group the only dwarf ellipticals are M 32, NGC 147, NGC 185 and NGC 205, all of which are satellites of M 31, while three of the five dwarf irregulars of comparable brightness (NGC 6822, IC 6822 and WLM) are free-floating within the Local Group potential (e.g. Mateo 1998; van den Bergh 1999). Beyond the Local Group, there are no known isolated dE galaxies within 8 Mpc (Karachentsev et al. 2004).

In a survey covering 900 deg² Binggeli, Tarengi & Sandage (1990) identify 179 dwarf galaxies, and claim that “*in the field there are virtually no isolated dEs, and that the few dEs outside of gravitationally bound systems are close satellites to massive giants.*” They find just one good candidate for an isolated dE, #179 in their dwarf catalogue. The reported location of this galaxy is covered by the SDSS, but no galaxy is found there, and it appears most likely to correspond to a $z = 0.08$ Sa galaxy 1 arcmin distant.

Dwarf ellipticals (including here dSphs) in contrast are the most numerous galaxy type in clusters, although unlike the field or within groups only a small fraction appear bound to massive galaxies (Ferguson 1992), the rest follow the general cluster potential. However, the ratio of dEs to giants is much greater in clusters than in groups or the field, and so not all cluster dEs can be accounted for by the accretion of “field” dEs (Conselice, Gallagher & Wyse 2001).

This clear segregation of passively-evolving dwarf galaxies places strong constraints on their formation and evolution, in particular as to the physical mechanisms that could cause them to cease forming stars. Most importantly, unlike massive galaxies for which their build-up through mergers appears fundamental in determining their star-formation history, we can rule out merging as a formation mechanism for passively-evolving dwarfs.

Galaxy merging is a stochastic process which occurs independently of the large-scale environment ($\gtrsim 1$ Mpc) of a galaxy (Hopkins et al. 2007a). This means that mergers take place in all environments¹, even in voids, as has been observed for interacting pairs (Alonso et al. 2006). This results in merger remnants being ubiquitous, as predicted by Hopkins et al. (2007a), and observed in the spatial distribution of post-starburst galaxies (Goto 2005; Hogg et al. 2006). This is most clearly demonstrated with the presence in all environments of passively-evolving, massive galaxies with old stellar populations, which in field regions make up $\gtrsim 50\%$ of the total population of massive galaxies, forming an equal interspersed mixture with younger star-forming galaxies (Figs. 3 and 4 from Paper I).

Hence dwarf galaxies which have undergone major mergers should also be ubiquitous, as Conselice (2006) shows that they have undergone on average about the same number of major mergers as massive galaxies since $z \sim 3$ (albeit at later epochs), yet we find no passively-evolving galaxies among the ~ 600 $-18 < M_r < -16$ dwarfs in the lowest density quartile. In addition, mergers cannot explain the observed strong segregation of dwarf galaxies, in particular the

¹ except in relaxed, rich clusters where encounter velocities are much higher than the internal velocity dispersions of galaxies, preventing their coalescence (Aarseth & Fall 1980)

presence of a massive galaxy should not affect the merging efficiency of a dwarf galaxy, or the observation that most dwarf star-forming galaxies in clusters are in the process of being transformed into passively-evolving galaxies, an environment where mergers are *now* strongly inhibited.

The ineffectiveness of mergers to permanently shut down star-formation in dwarf galaxies can be understood in the context of the current theoretical framework of galaxy evolution. Springel et al. (2005a) show through hydrodynamical simulations of mergers that although both models with and without black holes produce strong starbursts during the mergers followed by a decline in star-formation, in those models without black holes the remnants continue to form stars at a non-negligible rate. Given that the growth of central black holes during galaxy mergers are strongly regulated by the mass of the host galaxy, in low-mass galaxies the resultant black holes (if indeed there is one at all), based on the $M_{\text{BH}} - \sigma$ relation (Ferrarese & Ford 2005), are too small to power the quasar winds which would expel the remaining gas and shut down star-formation, as occurs in more massive systems. Indeed for merging galaxies with $\sigma = 80 \text{ km s}^{-1}$ Springel et al. (2005b) show that the effects of black hole growth are minimal on star-formation in the remnant galaxy, and the galaxy does not become passive as a result of the merger. Moreover, most dwarf galaxies ($M_B \gtrsim -18$) appear to host central compact stellar nuclei rather than a central supermassive black hole (Côté et al. 2006), consistent with our observation that the AGN fraction of galaxies falls to close to zero by $M_r \sim -18$ (§7). Even if a significant fraction of the available gas in the remnant is used up during the star-burst, the intrinsic low star-formation efficiency of low-mass galaxies and regulatory effects of supernovae feedback, plus the continuous infall and cooling of fresh gas from the halo along filaments (Kereš et al. 2005), ensures that the remaining gas is unlikely to be exhausted. Finally, the quasi-continuous low-level AGN activity that Croton et al. (2006) suggest could inhibit cooling of gas from the diffuse hot gaseous halo of massive galaxies and prevent subsequent star-formation in them, has in contrast little effect against the clumpy nature of the gas infalling along filamentary structures onto the dwarf merger remnants.

In Section 5 we find a significant anti-correlation (10σ) between the EW(H α) of dwarf star-forming galaxies and their local density, producing a systematic reduction of $\sim 30\%$ in the H α emission in high-density environments with respect to field values. We argue that this implies that the bulk of star-forming dwarf galaxies in groups and clusters are in the process of being slowly transformed into passive galaxies over long time-scales ($\gtrsim 1 \text{ Gyr}$), and is thus suggestive of suffocation (Balogh et al. 2000).

However, as discussed in Section 8 the long gas consumption time-scales predicted from Eq. 3 and observed by van Zee (2001) imply that even if deprived of further gas accretion through suffocation, star-formation in dwarf galaxies occurs at a sufficiently low rate that they are unlikely to have consumed all their gas by the present day. In low-mass dwarf galaxies ($M \lesssim 10^7 M_\odot$) as gas collapses and stars form, the resultant feedback from supernovae is able to drive out the remaining gas, temporarily shutting off star-formation, until the gas is able to cool and restart star-formation, resulting in episodic bursts of star-formation every $\sim 300 \text{ Myr}$ (Stinson et al. 2007). In more massive dwarf

galaxies, such as those studied here, SN feedback appears too inefficient to power galactic winds that could expel the remaining gas from dwarf galaxies, even during star-bursts (Mac Low & Ferrara 1999; Marcolini et al. 2006). Instead it seems that star-formation in dwarf galaxies appears strongly regulated and rather resilient over long time-scales. This quasi-continuous star-formation in dwarf galaxies seems to have been maintained since early epochs, as the global star-formation rates of galaxies with $M < 3 \times 10^{10} M_\odot$ have remained approximately constant since $z \sim 3$ (Panter et al. 2007).

A further difficulty for dEs being produced as the result of suffocation is that it does not affect the galaxy structurally, and so we should expect the surface brightness and luminosity to decrease in parallel as the stellar population evolves passively. However, the surface stellar mass densities of passively-evolving dwarf galaxies are 0.5 dex *higher* than their star-forming counterparts of the same stellar mass (Kauffmann et al. 2003b). Hence, if star-formation in dIrr galaxies were to simply be stopped, as in suffocation, the resultant surface densities would be too low in comparison to present-day dEs (Grebel et al. 2003). Equally, the metallicity of dIrrs are too low for their luminosity as compared with dEs, for them to be simply transformed by becoming passive (Grebel et al. 2003), while suffocation provides no means for the rotationally-supported dIrrs to lose their angular momentum to become the dEs where little or no signs of rotation ($\lesssim 5 \text{ km s}^{-1}$) are seen.

If gas cannot be exhausted through star-formation, expelled by supernovae feedback during star-bursts, or prevented from infalling and cooling through AGN feedback, the end of star-formation and gas removal in dwarf galaxies must come from external mechanisms, such as ram-pressure or tidal interactions (Marcolini et al. 2006).

When galaxies pass through the dense ICM of clusters or the gaseous halos of massive galaxies they feel an effective ram-pressure which, if able to overcome the gravitational attraction between the gas and the disk, is able to effectively strip the gas from the disk (for a review see van Gorkom 2004), according to the Gunn & Gott (1972) condition $\rho_{\text{ICM}} \nu_{\text{gal}}^2 > 2\pi G \Sigma_\star \Sigma_{\text{gas}}$, which has been shown to hold approximately from hydrodynamical simulations (e.g. Marcolini et al. 2003). Hence ram-pressure stripping should be more effective for lower mass, low-surface-brightness galaxies, galaxies on more eccentric orbits, and galaxies in richer environments (Hester 2006), such that while for massive galaxies ram-pressure stripping is only effective in the cores of rich clusters, dwarf galaxies can be completely stripped of their gas even in poor groups (Marcolini et al. 2003).

Moore et al. (1996) proposed that cluster spirals could be disrupted by “galaxy harassment”, whereby repeated close ($< 50 \text{ kpc}$) high-velocity ($> 1000 \text{ km s}^{-1}$) encounters with massive galaxies and the cluster’s tidal field cause impulsive gravitational shocks that damage the fragile disks of late-type disks, transforming them over a period of Gyr into spheroids. While $\sim L^\star$ spirals are relatively stable to the effects of harassment, suffering little or no mass loss, low surface brightness dwarf spirals with their shallower potentials may suffer significant mass losses (up to 90%) of both their stellar and dark matter components during harassment

(Moore et al. 1999), resulting in remnants resembling dwarf ellipticals (Mastropietro et al. 2005).

Dwarf spiral galaxies orbiting as satellites to massive galaxies may also be transformed into passively-evolving dEs through tidal interactions with the primary galaxy and ram-pressure stripping as they pass through its gaseous halo. Mayer et al. (2001) show that dwarf spirals orbiting a Milky Way type galaxy on eccentric orbits taking them within 50 kpc of the primary experience tidal shocks during their pericentre passages, that can cause significant mass loss (mostly of the outer gaseous halo and dark matter, but also of the stellar disk), formation of bar instabilities that channel gas inflows triggering nuclear star-bursts, and loss of angular momentum, resulting in their transformation over a period of ~ 5 Gyr an early-type dwarf. Mayer et al. (2006) indicate that while tidal stirring of disk dwarf galaxies can transform them into remnants that resemble dEs after a few orbits, ram-pressure stripping is required to entirely remove their gas component. Kravtsov, Gnedin & Klypin (2004) show that many dwarf satellites of Milky Way type galaxies have undergone significant mass loss through tidal stripping, and are able to reproduce the observed morphological segregation of dE and dIrr galaxies (Einasto et al. 1974), in which the dEs are those that have suffered significant tidal stripping.

As discussed above star-forming, late-type dwarf galaxies in clusters, groups or bound to massive galaxies can be transformed into dEs through a combination of ram-pressure stripping and tidal interactions. This is supported by the finding of significant populations of dEs in the Virgo cluster having blue central regions caused by recent or ongoing star-formation (Lisker et al. 2006), significant amounts ($\gtrsim 10^7 M_\odot$) of H I gas (Conselice et al. 2003), or clear disk features including spiral arms, bars or significant velocity gradients, with rotational velocities similar to dwarf irregulars of the same luminosity, and anisotropy parameters ($\nu/\sigma_m \gtrsim 1$) indicating stellar kinematics dominated by rotation rather than random motions (van Zee, Skillman & Haynes 2004). These populations are found predominately in the cluster outskirts and some have flat distributions of radial velocities, suggesting that they have been recently accreted by the cluster or are on high angular momentum orbits and therefore never go through the cluster core, while normal, non-rotating dEs are concentrated in the cluster core or in high-density clumps (Conselice et al. 2003; van Zee, Skillman & Haynes 2004; Lisker et al. 2007). In a similar H I study, this time of 11 dIrrs in the Virgo cluster, Lee, McCall & Richer (2003) find that five of them are gas deficient by a factor $\gtrsim 10$ with respect to field dIrrs at comparable oxygen abundances, and this gas deficiency correlates approximately with the X-ray surface brightness of the ICM. These gas-poor dIrrs have typical colours and luminosities of normal field dIrrs, indicating that their star-formation hasn't yet been affected, and suggesting that they have only recently encountered the ICM for the first time. In the Coma cluster Caldwell et al. (1993) and Poggianti et al. (2004) find that whereas bright post-starburst galaxies with k+a spectra are largely absent, there is a significant population of faint galaxies ($M_V > -18.5$) with k+a spectra, which appear associated with substructures in the ICM, the galaxies lying close to the edges of two infalling structures. This strongly suggests that the interaction with the ICM could

be responsible for rapidly quenching the star-formation in these galaxies, possibly after a starburst. These observations all point towards the *ongoing* transformation of late-type dwarf galaxies into passively-evolving dwarf ellipticals.

10 SUMMARY AND CONCLUSIONS

We present an analysis of star-formation in galaxies as a function of both luminosity and environment, in order to constrain the physical mechanisms that drive the star-formation histories of galaxies of different masses. In particular we wish to distinguish between mechanisms that are internal to the galaxy such as AGN feedback, gas consumption through star-formation and merging, and those related to the direct interaction of the galaxy with its surroundings including ram-pressure stripping and galaxy harassment.

For this analysis we use the NYU-VAGC low-redshift galaxy catalogues (Blanton et al. 2005c) taken from the SDSS DR4 spectroscopic dataset. Using a sample of 27 753 galaxies in the redshift range $0.005 < z < 0.037$ that is $\gtrsim 90\%$ complete to $M_r = -18.0$ we quantify the environment of each galaxy using an adaptive kernel method that for galaxies in groups or clusters resolves the local density on the scale of their host halo, while in field regions smooths over its 5-10 nearest neighbours. We use H α -emission as a gauge of the current star-formation in the galaxies and find that the EW(H α) distribution of galaxies is strongly bimodal, allowing them to be robustly separated into passively-evolving and star-forming populations about a value $\text{EW(H}\alpha) = 2\text{\AA}$. Aperture effects can strongly bias the estimates of star-formation rates based on spectra obtained through fibers which cover less than $\sim 20\%$ of the integrated galaxy flux, as is the case for SDSS spectra of galaxies in the redshift range of our sample (Kewley et al. 2005). For the massive galaxies in our sample with $M_r < -20$ we confirm that aperture effects are important finding a significant fraction of galaxies (mostly face-on spirals with prominent bulges) which are classified as passive from their spectra, but whose blue integrated NUV $- r$ colours indicate recent star-formation (Haines et al. 2007). Throughout the article we thus quantify and take full account of the effects of aperture biases on our results for the bright galaxies in our sample. For the dwarf galaxy population which represents our primary interest in this article, we find that aperture biases should not affect our results, in agreement with Brinchmann et al. (2004), due primarily to the absence of faint early-type spirals.

In the case of massive galaxies ($M \gtrsim 10^{10.5} M_\odot$; $M_r \lesssim -20$) we find only gradual trends of star-formation with environment, the fraction of passively-evolving galaxies increasing gradually with local density from $\sim 50\%$ to $\sim 70\%$ in high-density regions, the trend extending to the lowest density regions studied, well beyond the effects of cluster-related processes. For these galaxies only the large-scale galaxy density appears important for defining its star-formation history, and not its immediate neighbours or even whether it is within a cluster or group, implying that cluster-related processes are not the primary mechanisms by which massive galaxies become passive. The star-formation histories of massive galaxies appear to be predefined by the initial conditions in which they form, whereby in high-density re-

gions they are likely to form earlier and have more active merger histories than those in low-density regions, resulting in the observed gradual SF-density relations.

In contrast, the star-formation histories of dwarf galaxies ($\mathcal{M} \sim 10^{9.2} M_{\odot}$, $M_r \sim -18$) are strongly dependent on their local environment, the fraction of passively-evolving galaxies dropping from $\sim 70\%$ in dense environments, to $\sim 0\%$ in the rarefied field. Indeed for the lowest luminosity range covered ($-18 < M_r < -16$) none of the ~ 600 galaxies in the lowest density quartile are passively-evolving. The few passively-evolving dwarfs in field regions are strongly clustered around bright ($\gtrsim L^*$) galaxies, and throughout the SDSS sample we find no passively-evolving dwarf galaxies more than ~ 2 virial radii from a massive halo, whether that be a cluster, group or massive galaxy. This limit of around 2–2.5 virial radii corresponds to the maximum distance from a cluster or massive galaxy that a galaxy can rebound to having been previously subhalos within massive halos (Mamon et al. 2004; Diemand et al. 2007), and so it seems reasonable to believe that all passively-evolving dwarf galaxies are or have been satellites within a massive DM halo.

Our finding that passively-evolving dwarf galaxies are only found within cluster, groups or as satellites to massive galaxies indicates that internal processes or merging are not responsible for terminating star-formation in these galaxies. Instead the evolution of dwarf galaxies is primarily driven by the mass of their host halo, probably through the combined effects of tidal forces and ram-pressure stripping. We find a significant anti-correlation (10σ) between the EW(H α) of dwarf ($-19 < M_r < -18$) star-forming galaxies and local density, producing a a systematic reduction of $\sim 30\%$ in the H α emission in high-density regions with respect to field values. We argue that this implies that the bulk of star-forming dwarf galaxies in groups and clusters are currently in the process of being slowly transformed into passive galaxies. The transformation of dwarf galaxies solely through environmental processes results in the wide variety of star-formation histories observed in the local dwarf galaxy population (Mateo 1998).

Examining the fraction of passively-evolving galaxies as a function of both luminosity and local environment, we find that in high-density regions $\sim 70\%$ of galaxies are passively-evolving independent of luminosity. In the rarefied field, where environmental related processes are unlikely to be effective, however the fraction of passively-evolving galaxies is a strong function of luminosity, dropping from 50% for $M_r \lesssim -21$ to zero by $M_r = -18$. This strong luminosity dependence of the fraction of passive galaxies in field regions reflects with the systematic trend with increasing galaxy mass for star-formation histories to be driven by internal mechanisms as opposed to environmental processes. This transition from environmentally to internally-driven star-formation histories is likely due to a combination of factors:

- (i) the increasing efficiency and rapidity with which gas is converted into stars for more massive galaxies, resulting in gas-consumption time-scales for massive galaxies that are much shorter than the Hubble time;
- (ii) the mode for the accretion and cooling of fresh gas onto the galaxy from its surroundings. When galaxy halos reach a mass $\sim 10^{12} M_{\odot}$ expanding shocks heat infalling gas

to the virial temperature of the halo, producing a stable atmosphere of hot, diffuse gas which is vulnerable to feedback effects that can prevent the gas from cooling onto the galaxy (Kereš et al. 2005; Dekel & Birnboim 2006);

- (iii) AGN feedback in the form of quasar winds which can expel the remaining gas from a galaxy and/or the quasi-continuous low-level AGN activity that prevents cooling of the diffuse atmosphere of hot gas in massive galaxies. The observed paralleled increasing fractions of AGN and passive field galaxies with luminosity supports the importance of AGN feedback in shutting down star-formation in galaxies, a process which should become increasingly efficient with galaxy mass as the result of the tight $M_{\text{BH}} - \sigma$ relation;

- (iv) the increased susceptibility of low-mass galaxies to disruption by environmental effects such as tidal shocks and ram-pressure stripping due to their shallow potential wells.

The combined effect of these processes is to produce the observed bimodality in the global properties of galaxies about a characteristic mass of $\sim 3 \times 10^{10} M_{\odot}$ (Kauffmann et al. 2003a). However given that several models that treat each of these processes in diverse ways are qualitatively able to reproduce this bimodality (e.g. Menci et al. 2005; Bower et al. 2006; Croton et al. 2006; Cattaneo et al. 2006; Birnboim et al. 2007), it will be difficult to quantify the relative importance of the mechanisms for driving the star-formation histories of galaxies, although Hopkins et al. (2007b) show some observational tests that could distinguish between these models.

ACKNOWLEDGEMENTS

The authors thank Ivan Baldry, Agatino Rifatto and Eelco van Kampen for reading a draft version of the article, and the referee for useful comments regarding this work. CPH acknowledges the financial supports provided through the European Community’s Human Potential Program, under contract HPRN-CT-2002-0031 SISCO. AM acknowledges the INAF-Osservatorio Astronomico di Capodimonte for a grant. AG thanks her PhD supervisor Massimo Capaccioli.

Funding for the SDSS and SDSS-II has been provided by the Alfred P. Sloan Foundation, the Participating Institutions, the National Science Foundation, the U.S. Department of Energy, the National Aeronautics and Space Administration, the Japanese Monbukagakusho, the Max Planck Society, and the Higher Education Funding Council for England. The SDSS Web Site is <http://www.sdss.org/>.

The SDSS is managed by the Astrophysical Research Consortium for the Participating Institutions. The Participating Institutions are the American Museum of Natural History, Astrophysical Institute Potsdam, University of Basel, University of Cambridge, Case Western Reserve University, University of Chicago, Drexel University, Fermilab, the Institute for Advanced Study, the Japan Participation Group, Johns Hopkins University, the Joint Institute for Nuclear Astrophysics, the Kavli Institute for Particle Astrophysics and Cosmology, the Korean Scientist Group, the Chinese Academy of Sciences (LAMOST), Los Alamos National Laboratory, the Max-Planck-Institute for Astronomy (MPIA), the Max-Planck-Institute for Astrophysics (MPA), New Mexico State University, Ohio State University, University of Pittsburgh, University of Portsmouth, Princeton

University, the United States Naval Observatory, and the University of Washington.

This research has made use of the NASA/IPAC Extragalactic Database (NED) which is operated by the Jet Propulsion Laboratory, California Institute of Technology, under contract with the National Aeronautics and Space Administration.

The Millennium Run simulation used in this paper was carried out by the Virgo Supercomputing Consortium at the Computing Centre of the Max-Planck Society in Garching. The semi-analytic galaxy catalogue is publicly available at <http://www.mpa-garching.mpg.de/galform/agnpaper>

REFERENCES

- Aarseth S. J., Fall S. M., 1980, *ApJ*, 236, 43
- Adelman-McCarthy J. K., et al., 2006, *ApJS*, 163, 38
- Alonso S. M., Lambas D. G., Tissera P., Coldwell G., 2006, *MNRAS*, 367, 1029
- Baldry I. K., Glazebrook K., Brinkmann J., Ivezić Ž, Lupton R. H., Nichol R. C., Szalay A. S., 2004, *ApJ*, 600, 681
- Baldry I. K., Balogh M. L., Bower R. G., Glazebrook K., Nichol R. C., Bamford S. P., Budavari T., 2006, *MNRAS*, 373, 469 (BB06)
- Baldwin J. A., Phillips M. M., Terlevich R., 1981, *PASP*, 93, 5
- Balogh M. L., Morris S. L., Yee H. K. C., Carlberg R. G., Ellingson E., 1999, *ApJ*, 527, 54
- Balogh M. L., Navarro J. F. Morris S. L., 2000, *ApJ*, 540, 113
- Balogh M. L., et al., 2004a, *MNRAS*, 348, 1355 (B04)
- Balogh M. L., Baldry I. K., Nichol R., Miller C., Bower R., Glazebrook K., 2004b, *ApJL*, 615, 101 (BB04)
- Bardelli S., Pisani A., Ramella M., Zucca E., Zamorani G., 1998, *MNRAS*, 300, 589
- Bekki K., Couch W. J., Shioya Y., 2001, *PASJ*, 53, 395
- Bekki K., Couch W. J., Shioya Y., 2002, *ApJ*, 577, 651
- Bell E. F., de Jong R., 2001, *ApJ*, 550, 212
- Bell E. F., et al., 2004, *ApJ*, 608, 752
- Binggeli B., Tarenghi M., Sandage A., 1990, *A&A*, 228, 42
- Birnboim Y., Dekel A., Neistein E., 2007, preprint (astro-ph/0703435)
- Blanton M. R., Berlind A. A., Hogg D. W., 2006, preprint (astro-ph/0608353)
- Blanton M. R., et al., 2003a, *AJ*, 125, 2276
- Blanton M. R., et al., 2003b, *ApJ*, 594, 186
- Blanton M. R., et al., 2003c, *AJ*, 125, 2348
- Blanton M. R., et al., 2005a, *ApJ*, 629, 143
- Blanton M. R., et al., 2005b, *ApJ*, 631, 208
- Blanton M. R., et al., 2005c, *AJ*, 129, 2562
- Boselli A., Gavazzi G., 2006, *PASP*, 118, 517
- Boselli A., et al., 2006, *ApJ*, 651, 811
- Bower R. G., et al., 2006, *MNRAS*, 370, 645
- Brinchmann J., Charlot S., White S. D. M., Tremonti C., Kauffmann G., Heckman T., Brinkmann J., 2004, *MNRAS*, 351, 1151
- Bruzual A. G., Charlot S., 2003, *MNRAS*, 344, 1000
- Caldwell N., Rose J. A., Sharples R. M., Ellis R. S., Bower R. G., 1993, *AJ*, 106, 473
- Cardelli J. A., Clayton G. C., Mathis J. S., 1989, *ApJ*, 345, 245
- Cattaneo A., Dekel A., Devriendt J., Guideroni B., Blaizot J., 2006, *MNRAS*, 370, 1651
- Charlot S., Fall S. M., 2000, *ApJ*, 539, 718
- Chiosi C., Carraro G., 2002, *MNRAS*, 335, 335
- Christlein D., Zabludoff A. I., 2005, *ApJ*, 616, 192
- Cirasuolo M., et al., 2006, preprint(astro-ph/0609287)
- Conselice C. J., 2006, *ApJ*, 638, 686
- Conselice C. J., Gallagher J. S. III, Wyse R. F. G., 2001, *ApJ*, 559, 791
- Conselice C. J., O'Neill K., Gallagher J. S. III, Wyse R. F. G., 2003, *ApJ*, 591, 167
- Cooper M. C., et al., 2006, *MNRAS*, 370, 198
- Côté P., et al., 2006, *ApJS*, 165, 57
- Cox T. J., Di Matteo T., Hernquist L., Hopkins P. F., Robertson B., Springel V., 2006, *ApJ*, 643, 692
- Croton D. J., et al., 2006, *MNRAS*, 368, 11 (C06)
- Davoodi P., et al., 2006, *MNRAS*, 371, 1113
- Dekel A., Birnboim Y., 2006, *MNRAS*, 368, 2
- de Lapparent V., 2003, *A&A*, 408, 845
- Desai V., et al., 2007, *ApJ*, 660, 1151
- de Vaucouleurs G., 1961, *ApJS*, 5, 233
- Diemand J., Kuhlen M., Madau P., 2007, preprint (astro-ph/0703337)
- di Matteo T., Springel V., Hernquist L., 2005, *Nature*, 433, 604
- Dressler A., 1980, *ApJ*, 236, 772
- Dressler A., et al., 1997, *ApJ*, 490, 577
- Driver S. P., et al., 2006, *MNRAS*, 368, 414
- Einasto J., Saar E., Kaasik A., Chernin A. D., 1974, *Nature*, 252, 111
- Ferguson H. C., 1992, *MNRAS*, 255, 389
- Ferguson H. C., Binggeli B., 1994, *A&ARv*, 6, 67
- Ferrarese L., Ford, H., 2005, *Space Science Reviews*, 116, 523
- Ferrarese L., et al., 2006, *ApJS*, 164, 334
- Fujita Y., Nagashima M., 1999, *ApJ*, 516, 619
- Gebhardt K., et al., 2000, *ApJL*, 539, 13
- Girardi M., Giuricin G., Mardirossian F., Mezzetti M., Boschin W., 1998, *ApJ*, 505, 74
- Glazebrook K., et al., 2004, *Nature*, 430, 181
- Gómez P., et al., 2003, *ApJ*, 584, 210
- Goto T., 2005, *MNRAS*, 357, 937
- Goto T., et al., 2003, *PASJ*, 55, 757
- Gottlöber S., Klypin A., Kravtsov A. V., 2001, *ApJ*, 546, 223
- Graham A. W., Driver S., 2007, *ApJ*, 655, 77
- Gray M. E., Wolf C., Meisenheimer K., Taylor A., Dye S., Borch A., Kleinheinrich M. 2004, *MNRAS*, 357, L73
- Grebel E. K., Gallagher J. S., Harbeck D., 2003, *AJ*, 125, 1926
- Gunn J. E., Gott J. R., 1972, *ApJ*, 176, 1
- Haehnelt M. G., Natarajan P., Rees M. J., 1998, *MNRAS*, 300, 817
- Haines C. P., Campusano L. E., Clowes R. G., 2004a, *A&A*, 421, 157
- Haines C. P., Mercurio A., Merluzzi P., La Barbera F., Massarotti M., Busarello G., Girardi M., 2004b, *A&A*, 425, 783
- Haines C. P., Merluzzi P., Mercurio A., Gargiulo A., Kru-

- sanova N., Busarello G., La Barbera F., Capaccioli M., 2006a, *MNRAS*, 371, 55
- Haines C. P., La Barbera F., Mercurio A., Merluzzi P., Busarello G., 2006b, *ApJL*, 647, 21 (Paper I)
- Haines C. P., Gargiulo A., Merluzzi P., 2007, in preparation (Paper III)
- Häring N., Rix H.-W., 2004, *ApJL*, 604, 89
- Hao L., et al., 2005, *AJ*, 129, 1783
- Heavens A., Panter B., Jimenez R., Dunlop J., 2004, *Nature*, 428, 625
- Hester J. A., 2006, *ApJ*, 647, 910
- Hogg D. W., Masjedi M., Berlind A. A., Blanton M. R., Quintero A. D., Brinkmann J., 2006, *ApJ*, 650, 763
- Hopkins A. M., et al., 2003, *ApJ*, 599, 971
- Hopkins P. F., Hernquist L., Cox T. J., Di Matteo T., Robertson B., Springel V., 2006a, *ApJS*, 163, 1
- Hopkins P. F., Hernquist L., Cox T. J., Robertson B., Springel V., 2006b, *ApJS*, 163, 50
- Hopkins P. F., Hernquist L., Cox T. J., Kereš D., 2007a, preprint (astro-ph/0706.1243)
- Hopkins P. F., Cox T. J., Kereš D., Hernquist L., 2007b, preprint (astro-ph/0706.1246)
- Hubble E. P., 1926, *ApJ*, 64, 321
- Hubble E. P., 1936, *The Realm of the Nebulae*. Yale University Press, New Haven
- Hubble E. P., Humason M. L., 1931, *ApJ*, 71, 43
- Jungwiert B., Combes F., Palous J., 2001, *A&A*, 376, 85
- Kapferer W., et al., 2007, *A&A*, 466, 813
- Karachentsev I. D., 2005, *AJ*, 129, 178
- Karachentsev I. D., Karachentseva V. E., Huchtmeier W. K., Makarov D. I., 2004, *AJ*, 127, 2031
- Kauffmann G., White S. D. M., Guideroni B., 1993, *MNRAS*, 264, 201
- Kauffmann G., et al., 2003a, *MNRAS*, 341, 33 (K03)
- Kauffmann G., et al., 2003b, *MNRAS*, 341, 54
- Kauffmann G., et al., 2003c, *MNRAS*, 346, 1055
- Kauffmann G., et al., 2004, *MNRAS*, 353, 713
- Kauffmann G., et al., 2006, *MNRAS*, 367, 1408
- Kennicutt R. C. Jr., 1998, *ARA&A*, 36, 189
- Kereš D., Katz N., Weinberg D. H., Davé R., 2005, *MNRAS*, 363, 2
- Kewley L. J., Dopita M. A., Sutherland R. S., Heisler C. A., Trevena J., 2001, *ApJ*, 556, 121
- Kewley L. J., Jansen R. A., Geller M. J., 2005, *PASP*, 117, 227
- Kewley L. J., Groves B., Kauffmann G., Heckman T., 2006, *MNRAS*, 372, 961
- Koopmann R. A., Kenney J. D. P., 2004, *ApJ*, 613, 851
- Kravtsov A. V., Gnedin O. Y., Klypin A. A., 2004, *ApJ*, 609, 482
- Kriek M., et al., 2006, *ApJL*, 649, 71
- Lacey C., Cole S., 1993, *MNRAS*, 262, 627
- Larson R. B., Tinsley B. M., Caldwell C. N., 1980, *MNRAS*, 237, 692
- Lee H., McCall M. L., Richer M. G., 2003, *AJ*, 125, 2975
- Lemson G., Kauffmann G., 1999, 302, 111
- Lewis I., et al., 2002, *MNRAS*, 334, 673
- Lisker T., Glatt K., Westera P., Grebel E. K., 2006, *AJ*, 132, 2432
- Lisker T., Grebel E. K., Binggeli B., Glatt K., 2007, *ApJ*, 660, 1186
- Mac Low M.-M., Ferrara A., 1999, *ApJ*, 513, 142
- Mahdavi A., Geller M. J., 2004, *ApJ*, 607, 202
- Mamon G. A., Sanchis T., Salvador-Solé E., Solanes J. M., 2004, *A&A*, 414, 445
- Marcolini A., Brighenti F., D’Ercole A., 2003, *MNRAS*, 345, 1329
- Marcolini A., D’Ercole A., Brighenti F., Recchi S., 2006, *MNRAS*, 371, 643
- Martin C. L., Kennicutt R. C., 2001, *ApJ*, 555, 301
- Martini P., Kelson D. D., Kim E., Mulchaey J. S., Athey A. A., 2006, *ApJ*, 644, 116
- Mastropietro C., Moore B., Mayer L., Debattista V. P., Piffaretti R., Stadel J. 2005, *MNRAS*, 364, 607
- Mateo M., 1998, *ARA&A*, 36, 435
- Mateus A., Sodré L., Cid Fernandes R., Stasińska G., Schoenell W., Gomes J. M., 2006, *MNRAS*, 370, 721
- Mateus A., Sodré L., Cid Fernandes R., Stasińska G., 2007, *MNRAS*, 374, 1457
- Mathews W. G., Brighenti F., 2003, *ARA&A*, 41, 191
- Maulbetsch C., Avila-Reese V., Colin P., Gottlöber S., Khalatyan A., Steinmetz M., 2007, *ApJ*, 654, 53
- Mayer L., Governato F., Colpi M., Moore B., Quinn T., Wadsley J., Stadel J., Lake G., 2001, *ApJ*, 559, 754
- Mayer L., Mastropietro C., Wadsley J., Stadel J., Moore B., 2006, *MNRAS*, 369, 1021
- Menci N., Fontana A., Giallongo E., Salimbeni S., 2005, *ApJ*, 632, 49
- Mercurio A., Merluzzi P., Haines C. P., Gargiulo A., Kruzanova N., La Barbera F., Busarello G., Capaccioli M., Covone G., 2006, *MNRAS*, 368, 109
- Merlin E., Chiosi C., 2006, *A&A*, 457, 437
- Miller C. J., et al., 2003, *ApJ*, 597, 142
- Moore B., Katz N., Lake G., Dressler A., Oemler A. Jr., 1996, *Nature*, 379, 613
- Moore B., Lake G., Quinn T., Stadel J., 1999, *MNRAS*, 364, 465
- Morgan W. W., 1958, *PASP*, 70, 415
- Moustakas J., Kennicutt R. C. Jr., Tremonti, C. A., 2006, *ApJ*, 642, 775
- Naab T., Johansson P. H., Ostriker J. P., Efstathiou G., 2007, *ApJ*, 658, 710
- Nelan J. E., Smith R. J., Hudson M. J., Wegner G. A., Lucey J. R., Moore S. A. W., Quinney S. J., Suntzeef N. B., 2005, *ApJ*, 632, 137
- Noeske K. G., et al. 2007a, *ApJL*, 660, L43
- Noeske K. G., et al. 2007b, *ApJL*, 660, L47
- Nolan L. A., Raychaudhury S., Kabán A., 2007, *MNRAS*, 375, 381
- Panter B., Jimenez R., Heavens A. F., Charlot S., 2007, *MNRAS*, 378, 1550
- Panuzzo P., et al., 2007, *ApJ*, 656, 206
- Pisani A., 1993, *MNRAS*, 265, 706
- Pisani A., 1996, *MNRAS*, 278, 697
- Poggianti B. M., Bridges T. J., Komiyama Y., Yagi M., Carter D., Mobasher B., Okamura S., Kashikawa N., 2004, *ApJ*, 601, 197
- Popesso P., Böhringer H., Brinkmann J., Voges W., York D. G., 2004, *A&A*, 423, 449
- Quadri R., et al., 2007, *ApJ*, 654, 138
- Renzini A., 2006, *ARA&A*, 44, 141
- Rigby J. R., Rieke G. H., Donley J. L., Alonso-Herrero A., Pérez-González P. G., 2006, *ApJ*, 645, 11
- Rines K., Diaferio A., 2006, *AJ*, 132, 1275

- Rines K., Geller M. J., Kurtz M. J., Diaferio A., 2005, *AJ*, 130, 1482 (R05)
- Robertson B., Cox T. J., Hernquist L., Franx M., Hopkins P. F., Martini P., Springel V., 2006, *ApJ*, 641, 21
- Roediger E., Hensler G., 2005, *A&A*, 433, 875
- Roettiger K., Burns J. O., Loken C., 1996, *ApJ*, 673, 451
- Rossa J., et al., 2006, *AJ*, 132, 1074
- Ruderman J. T., Ebeling H., 2005, *ApJL*, 623, 81
- Sales L. V., Navarro J. F., Abadi M. G., Steinmetz M., 2007, preprint (astro-ph/0704.1770)
- Scannapieco C., Tissera P. B., White S. D. M., Springel V., 2006, *MNRAS*, 371, 1125
- Schlegel D. J., Finkbeiner D. P., Davis M., 1998, *ApJ*, 500, 525
- Schmidt M., 1959, *ApJ*, 129, 243
- Silk J., Rees M., 1998, *A&A*, 334, L1
- Silverman B. W., 1986, *Density Estimation for Statistics and Data Analysis*. Chapman and Hall, London
- Smith G. P., Treu T., Ellis R. S., Moran S. M., Dressler A., 2005, *ApJ*, 620, 78
- Smith R. J., Hudson M. J., Lucey J. R., Nelán J. E., Wegner G. A., 2006, *MNRAS*, 369, 1419
- Söchtig I. K., Clowes R. G., Campusano L. E., 2004, *MNRAS*, 1241, 1254
- Solanes J. M., Manrique A., García-Gómez C., González-Casado G., Giovanelli R., Haynes M. P., 2001, *ApJ*, 548, 97
- Sorrentino G., Antonuccio-Delogu V., Rifatto A., 2006, *A&A*, 460, 673
- Sorrentino G., Radovich M., Rifatto A., 2006, *A&A*, 451, 809
- Springel V., di Matteo T., Hernquist L., 2005a, *MNRAS*, 361, 776
- Springel V., di Matteo T., Hernquist L., 2005b, *ApJL*, 620, 79
- Springel V., et al., 2005c, *Nat*, 435, 629
- Stoughton C., et al., 2002, *AJ*, 123, 485
- Stinson G. S., Dalcanton J. J., Quinn T., Kaufmann T., Wadsley J., 2007, preprint (astro-ph/0705.4494)
- Strateva I., et al., 2001, *AJ*, 122, 1861
- Strauss M. A., et al., 2002, *AJ*, 124, 1810
- Struck C., 2006, in ed. J. W. Mason, *Astrophysics Update 2*. Springer Verlag, Heidelberg, p. 115
- Tanaka M., Goto T., Okamura S., Shimasaku K., Brinkmann, J., 2004, *AJ*, 128, 2677 (T04)
- Tanaka M., et al., 2005, *MNRAS*, 362, 268
- Tassis K., Kravtsov A. V., Gnedin N. Y., 2006, preprint (astro-ph/0609763)
- Thomas D., Maraston C., Bender R., Mendes de Oliveira C., 2005, *ApJ*, 621, 673
- Toomre A., 1977, in Tinsley B. M., Larson R. B., eds, *Evolution of Galaxies and Stellar Populations*. Yale Univ. Obs., New Haven, p. 401
- Tremonti C. A., et al., 2004, *ApJ*, 613, 898
- Treu T., Ellis R. S., Kneib J.-P., Dressler A., Smail I., Czoske O., Oemler A., Natarajan P., 2003, *ApJ*, 591, 53
- van den Bergh S., 1976, *ApJ*, 206, 883
- van den Bergh S., 1999, *A&A Review*, 9, 273
- van Dokkum P., van der Marel R. P., 2007, *ApJ*, 655, 30
- van Gorkom J., 2004, in eds. Mulchaey J. S., Dressler A., Oemler A., *Clusters of Galaxies: Probes of Cosmological Structure and Galaxy Evolution*. Cambridge University Press, New York, p. 306
- van Zee L., 2001, *AJ*, 121, 2003
- van Zee L., Skillman E. D., Haynes M. P., 2004, *AJ*, 128, 121
- Vogt N., Haynes M. P., Giovanelli R., Herter T., 2004, *AJ*, 127, 3300
- Vollmer B., Cayatte V., Balkowski C., Duschl W. J., 2001, *ApJ*, 561, 708
- Wehner E. H., Harris W. E., 2006, *ApJL*, 644, 17
- Weinmann S. M., van den Bosch F. C., Yang X., Mo H. J., 2006a, *MNRAS*, 366, 2
- Weinmann S. M., van den Bosch F. C., Yang X., Mo H. J., Croton D. J., Moore B., 2006b, *MNRAS*, 372, 1161
- White S. D. M., Rees M. R., 1978, *MNRAS*, 183, 341
- White R. A., Bliton M., Bhavsar S. P., Bornmann P., Burns J. O., Ledlow M. J., Loken C., 1999, *AJ*, 118, 2014
- Willmer C. N. A. et al., 2006, 647, 853
- Wolf C., Gray M. E., Meisenheimer K., 2005, *A&A*, 443, 435
- Yang X., Mo H. J., van den Bosch F. C., Jing Y. P., 2005, *MNRAS*, 356, 1293
- York D. G. et al., 2000, *AJ*, 120, 1579
- Zehavi I. et al., 2005, *ApJ*, 630, 1

APPENDIX A: TESTING OF THE DENSITY ESTIMATOR

We test the efficiency of this density estimation algorithm, by applying it to the public galaxy catalogues from the Millennium simulation (Springel et al. 2005c; Croton et al. 2006). These simulations cover a $(500 h^{-1} \text{Mpc})^3$ volume producing a galaxy catalogue complete to $M_r = -17.4$ containing some 9 million galaxies, for which positions, peculiar velocities, absolute magnitudes in each of the SDSS filters, stellar masses are all provided. From this, we consider $61\,981 M_r < -18$ galaxies from a subregion of volume $200 \times 200 \times 100 \text{ Mpc}^3$. We estimate the local density of each galaxy in physical space, $\rho(3D)$, by applying the adaptive kernel method, representing each galaxy by a spherically-symmetric Gaussian kernel whose width is equal to the distance to its 5th nearest neighbour. Galaxy groups and clusters are identified through a percolation analysis using a friends-of-friends algorithm with a linking length equal to 0.2 times the mean interparticle separation. For each group containing four or more members, the velocity dispersion (σ_v) and virial radius (R_{vir}) are calculated following Girardi et al. (1998). For each galaxy we combine the position and peculiar velocity in the z -direction to create a redshift, producing a volume-limited redshift catalogue, to which we apply exactly the same adaptive kernel method as for the SDSS data, representing each galaxy by a Gaussian kernel of transverse width defined by the distance to its 3rd nearest neighbour within 500 km s^{-1} and of width 500 km s^{-1} in the radial/redshift direction. The resultant distribution of local galaxy densities, ρ , is shown in the left panel Fig.A1 by the solid black lines. It shows a peak at ~ 0.2 , which is close to the global mean $M_r < -18$ galaxy density of $0.11 \text{ Mpc}^{-2} (500 \text{ km s}^{-1})^{-1}$, and a long tail extending to high densities.

To examine the efficiency of this density estimator in identifying galaxies within groups the red filled histogram

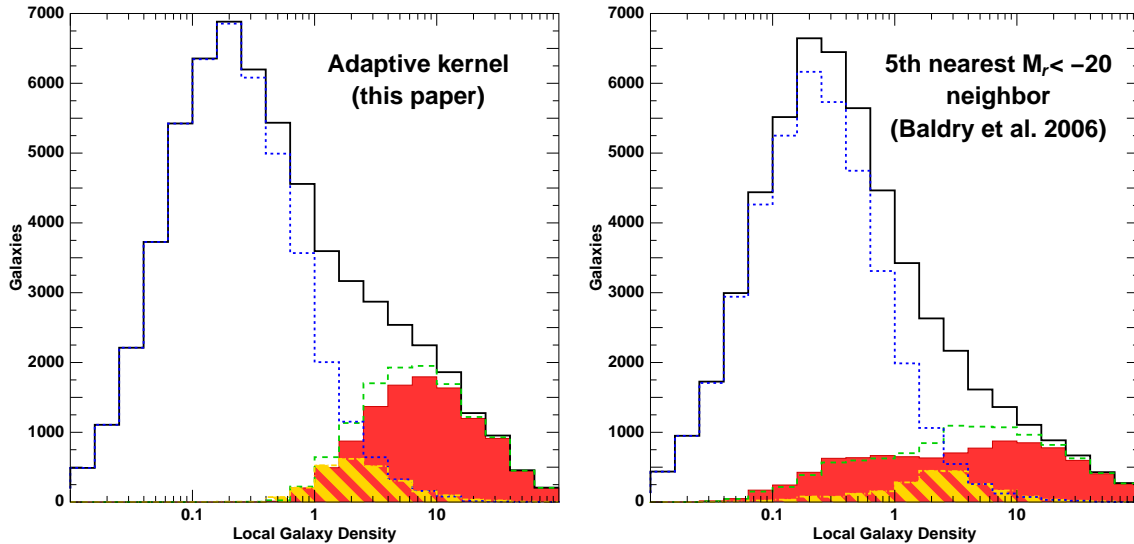


Figure A1. Distribution of “observed” local galaxy densities from Millennium simulation as calculated using the adaptive kernel algorithm (left) and based on the distance of the 5th nearest neighbour with $M_r < -20$ (Balogh et al. 2004a; Baldry et al. 2006). The histograms show the local density distributions of all $M_r < -18$ galaxies (black solid lines), those galaxies within groups containing 4 or more members (red filled histogram), those galaxies within $1 R_{\text{vir}}$ (green dashed lines), $0.8 < (r/R_{\text{vir}}) < 1.2$ (yellow hatched histogram with dot-dashed lines), and more than $2 R_{\text{vir}}$ (blue short-dashed lines) from the nearest group or cluster.

shows the density distribution of galaxies that were identified by the percolation analysis to belong to a group containing four or more members. Alternatively, the green-dashed histogram shows the density distribution of those galaxies within the virial radius of a group containing four or more galaxies. In both cases, the observed local galaxy density of group galaxies are strongly biased to high densities with $\rho > 1$, while *no* group galaxy has $\rho < 0.5$. The yellow hatched histogram shows the density distribution of those galaxies in the transition regions between group and field environments having $0.8 < (r/R_{\text{vir}}) < 1.2$. Galaxies in these transition regions have local densities in the range $1 \lesssim \rho \lesssim 4$. Finally, the blue short-dashed histogram shows those galaxies in isolated field regions more than two virial radii from the nearest group, and hence are unlikely to have encountered the group environment during their evolution or be affected by group/cluster-related physical processes. As expected, they are observed to have low local densities with $\rho \lesssim 1$.

The left panel of Fig. A1 demonstrates the efficiency of this density estimator in identifying group and isolated field galaxies, in particular the latter. By selecting galaxies with $\rho < 0.5$ we can be sure of obtaining a sample of field galaxies, the vast majority ($> 97\%$) at $> 2 R_{\text{vir}}$, and with no contamination from any galaxies belonging to groups or clusters, even those containing as few as four galaxies. Considering instead those galaxies with $\rho < 1.0$, $> 95\%$ still have $> 2 R_{\text{vir}}$, while only 0.7% lie within the virial radius of a group. In contrast, $\sim 60\%$ of $\rho > 1.0$ and $\sim 90\%$ of $\rho > 4$ galaxies are at $< 1 R_{\text{vir}}$.

For comparison the right panel of Fig. A1 shows the same density distributions of field and group galaxies brighter than $M_r = -18$ using the nearest neighbour algorithm as applied by BB04 and BB06 who estimate the local density on the basis of the projected distance to the 5th nearest neighbour that is brighter than $M_r = -20$ and has a ra-

dial velocity within 1000 km s^{-1} of each galaxy. The overall density distributions are quite similar, as although there are three times fewer $M_r < -20$ galaxies than $M_r < -18$ galaxies, the recession velocity range over which the projected density is estimated is quadruple that used for the adaptive kernel estimator (2000 km s^{-1} instead of 500 km s^{-1}). The most important difference between the two estimators is the much broader density distribution of group galaxies (red filled histogram) for the nearest neighbour algorithm, which extends to much lower “observed” densities than our approach. Even at the lowest densities studied by BB04 and BB06, corresponding to $\Sigma_5 \simeq 0.1$, $\sim 5\%$ of the galaxies are group members, and hence could have been affected by group-related environmental processes. Equally, Σ_5 does not appear very sensitive to the position of a galaxy within a halo, as is apparent by the densities of those galaxies at and around the virial radius of groups being covering a wide range of values of Σ_5 and peaking at a mid-range value for galaxies within groups, rather than that obtained from the adaptive kernel approach where galaxies near the virial radius have generally the lowest densities of those galaxies in groups. The value of Σ_5 is instead most sensitive to the *mass* of the nearest massive halo, rather than whether a galaxy is inside or outside that halo.

To fairly compare the efficiency of the adaptive kernel estimator against nearest neighbour approaches, we retested the nearest neighbour algorithm using the same $M_r < -18$ datasets, varying the number of neighbours used over the range 3–10, and the velocity range used to select neighbours from 400 to 1000 km s^{-1} . We define the efficiency of the density estimators in two ways: firstly in terms of the rank correlation between the observed projected density and the actual physical 3-dimensional galaxy density $\rho(3D)$; and secondly its sensitivity to the position of the galaxy within a halo, as measured by the correlation with the distance r to the nearest massive halo (containing four or more galaxies)

Table A1. Comparison of efficiencies of density estimators

Method used	No. of neighbours	Magnitude limit	Velocity range (km s ⁻¹)	Spearman rank correlation	
				$\rho(3D)$	r/R_{vir}
AK	3	$M_r < -18$	500	0.891	-0.800
NN	3	$M_r < -18$	500	0.849	-0.744
NN	5	$M_r < -18$	500	0.896	-0.774
NN	8	$M_r < -18$	500	0.890	-0.786
NN	10	$M_r < -18$	500	0.877	-0.789
NN	5	$M_r < -18$	1000	0.856	-0.766
NN	5	$M_r < -18$	800	0.872	-0.772
NN	5	$M_r < -18$	600	0.889	-0.775
NN	5	$M_r < -18$	500	0.896	-0.774
NN	5	$M_r < -18$	400	0.898	-0.766
NN	5	$M_r < -20$	1000	0.785	-0.741

scaled by the virial radius R_{vir} . We measure the strengths of these correlations through the Spearman rank correlation test as presented in Table A1. Firstly, varying the numbers of neighbours used to estimate the local density, we find that Σ_5 is the most sensitive to the actual physical local density $\rho(3D)$, while Σ_{10} is the most sensitive to the position of the galaxy within the halo (for neighbours within 500 km s⁻¹). Secondly, varying the velocity range over which neighbours are selected, we find that a range of 400 km s⁻¹ is most sensitive to the physical density, while a range of 600 km s⁻¹ is the most sensitive to the position of the galaxy within the halo. These confirm that using a range of 500 km s⁻¹ is the optimal general purpose value for estimating the local density of galaxies (at least for samples extending to $M_r \sim -18$, while the commonly used value of 1000 km s⁻¹ is much less efficient due to contamination of projected background galaxies. Comparing our adaptive kernel estimator to the nearest neighbour algorithm, we find that it is always more sensitive to the position of the galaxy within a halo, and is only marginally less efficient than the optimal choice of parameters for the nearest neighbour algorithm (Σ_5). The adaptive kernel estimator we have adopted is at least as efficient as any comparable nearest neighbour algorithms, and is particularly sensitive to the position of a galaxy within a halo, which is likely to be the most important aspect of the environment in terms of affecting its evolution (Lemson & Kauffmann 1999).

In comparison we note that the particular algorithm used by BB04, BB06 is significantly less sensitive to both the $\rho(3D)$ and the position of the galaxy within the host halo (last row of Table A1). These differences reflect the practical issue of the density of information used to characterize the environment of a galaxy. By measuring the local environment using just $M_r < -20$ galaxies, the density of information is much sparser, making it that much less sensitive to effects on the scales of poor groups, which may contain three or less $M_r < -20$ galaxies. However, a volume of the universe can be covered that is a factor ten larger than is possible using our approach which is limited by the necessity of being complete to $M_r = -18$, and indeed for galaxies brighter than $\sim M^*$ our analysis of their environ-

mental trends are strongly limited by the small sample size. In addition, in the volume covered by our analysis, the only rich structures (with $\sigma_v \gtrsim 500$ km s⁻¹) are the supercluster associated with the rich cluster Abell 2199 studied in Paper I, and Abell 1314, limiting our ability to follow the environmental trends to the highest densities.

The adaptive kernel method has the added advantage of being able to be used as a group-finder (e.g. Bardelli et al. 1998; Haines et al. 2004a), by identifying groups and clusters as local maxima in the galaxy density function $\rho(\mathbf{x}, z)$. A comparison of the groups identified in the Millennium simulation from a percolation analysis, finds that all such groups containing four or more members are marked as clear local maxima in the luminosity-weighted density maps. Unlike group finding algorithms based on a percolation analysis, the adaptive kernel approach is also able to efficiently define substructures that are the natural consequence of the hierarchical merging of galaxy groups and clusters.